DTIC FILE COPY

AD-A226 250

REPORT DOCUMENTATION PAGE

Form Approved
OMB No. 0704-0188

1. AGENCY USE ONLY (Leave blank)	2. REPORT DATE	3. REPORT TYPE AND DATES COVERED
		Final Report/1 Jun 84-30 Sep 86

TITLE AND SUBTITLE

MAGNETOFLUIDMECHANICS

5. FUNDING NUMBERS

61102F/2301/A7

AUTHOR(S)

S. T. Demetriades, D. A. Oliver
and C. D. Maxwell

PERFORMING ORGANIZATION NAME(S) AND ADDRESS(ES)

STD Research Corporation
P. O. Box "C"
Arcadia, CA 91006

8. PERFORMING ORGANIZATION REPORT NUMBER

AFOSR-TR- 90 0860

SPONSORING/MONITORING AGENCY NAME(S) AND ADDRESS(ES)

AFOSR/NP
Bolling AFB DC 20332-6448

10. SPONSORING/MONITORING AGENCY REPORT NUMBER

F49620-84-C-0068

11. SUPPLEMENTARY NOTES

12a. DISTRIBUTION/AVAILABILITY STATEMENT

Approved for public release; distribution is unlimited.

12b. DISTRIBUTION CODE

13. ABSTRACT (Maximum 200 words)

The magnetic field equations of a conducting fluid slab under steady flow were found subject to the boundary condition that the induced magnetic field immediately in front of the fluid exactly oppose the corresponding induced magnetic field at the trailing edge of the fluid so as to maintain divergence of B equal to O.) (See Demetriades, et al, AIAA J, Vol 23, No. 11, pp 1813-1814). Experimentally, MHD generators with rocket type combustors were shown to be a viable form of portable, high peak power sources. (See Maxwell and Demetriades, AIAA J., Vol 7, No 1, p 474).

14. SUBJECT TERMS

magnetofluidmechanics, thermodynamics, electromagnetic. (40)

15. NUMBER OF PAGES

48

16. PRICE CODE

17. SECURITY CLASSIFICATION OF REPORT	18. SECURITY CLASSIFICATION OF THIS PAGE	19. SECURITY CLASSIFICATION OF ABSTRACT	20. LIMITATION OF ABSTRACT
UNCLASSIFIED	UNCLASSIFIED	UNCLASSIFIED	UL SAR

GENERAL INSTRUCTIONS FOR COMPLETING SF 298

The Report Documentation Page (RDP) is used in announcing and cataloging reports. It is important that this information be consistent with the rest of the report, particularly the cover and title page. Instructions for filling in each block of the form follow. It is important to stay ***within the lines*** to meet ***optical scanning requirements.***

Block 1. Agency Use Only *(Leave blank)*.

Block 2. Report Date. Full publication date including day, month, and year, if available (e.g. 1 Jan 88). Must cite at least the year.

Block 3. Type of Report and Dates Covered. State whether report is interim, final, etc. If applicable, enter inclusive report dates (e.g. 10 Jun 87 - 30 Jun 88).

Block 4. Title and Subtitle. A title is taken from the part of the report that provides the most meaningful and complete information. When a report is prepared in more than one volume, repeat the primary title, add volume number, and include subtitle for the specific volume. On classified documents enter the title classification in parentheses.

Block 5. Funding Numbers. To include contract and grant numbers; may include program element number(s), project number(s), task number(s), and work unit number(s). Use the following labels:

C	- Contract	PR	- Project
G	- Grant	TA	- Task
PE	- Program Element	WU	- Work Unit Accession No.

Block 6. Author(s). Name(s) of person(s) responsible for writing the report, performing the research, or credited with the content of the report. If editor or compiler, this should follow the name(s).

Block 7. Performing Organization Name(s) and Address(es). Self-explanatory.

Block 8. Performing Organization Report Number. Enter the unique alphanumeric report number(s) assigned by the organization performing the report.

Block 9. Sponsoring/Monitoring Agency Name(s) and Address(es). Self-explanatory.

Block 10. Sponsoring/Monitoring Agency Report Number. *(If known)*

Block 11. Supplementary Notes. Enter information not included elsewhere such as: Prepared in cooperation with...; Trans. of...; To be published in.... When a report is revised, include a statement whether the new report supersedes or supplements the older report.

Block 12a. Distribution/Availability Statement. Denotes public availability or limitations. Cite any availability to the public. Enter additional limitations or special markings in all capitals (e.g. NOFORN, REL, ITAR).

- DOD - See DoDD 5230.24, "Distribution Statements on Technical Documents."
- DOE - See authorities.
- NASA - See Handbook NHB 2200.2.
- NTIS - Leave blank.

Block 12b. Distribution Code.

- DOD - Leave blank.
- DOE - Enter DOE distribution categories from the Standard Distribution for Unclassified Scientific and Technical Reports.
- NASA - Leave blank.
- NTIS - Leave blank.

Block 13. Abstract. Include a brief *(Maximum 200 words)* factual summary of the most significant information contained in the report.

Block 14. Subject Terms. Keywords or phrases identifying major subjects in the report.

Block 15. Number of Pages. Enter the total number of pages.

Block 16. Price Code. Enter appropriate price code *(NTIS only)*.

Blocks 17. - 19. Security Classifications. Self-explanatory. Enter U.S. Security Classification in accordance with U.S. Security Regulations (i.e., UNCLASSIFIED). If form contains classified information, stamp classification on the top and bottom of the page.

Block 20. Limitation of Abstract. This block must be completed to assign a limitation to the abstract. Enter either UL (unlimited) or SAR (same as report). An entry in this block is necessary if the abstract is to be limited. If blank, the abstract is assumed to be unlimited.

FINAL REPORT

F49620-84-C-0068

MAGNETOFLUIDMECHANICS

STD Research Corporation

S. T. Demetriades

D. A. Oliver

C. D. Maxwell

Chapter accepted for publication in the *Handbook of Fluid Dynamics and Fluid Machinery*, edited by Prof. Allen E. Fuhs, John Wiley and Sons, Publishers, 605 Third Ave., New York, New York 10158.

MAGNETOFLUIDMECHANICS*

by

S. T. Demetriades, D. A. Oliver, and C. D. Maxwell

1. INTRODUCTION

Any attempt to go past the limits of specific energy (energy per unit mass) imposed by the chemical bond in the production, generation, containment, manipulation, conversion or utilization of energy or energetic fluids requires the application of the principles of magneto- and electrofluidmechanics. As examples, we may consider the generation of electricity from gases at temperatures above 2000° K, the acceleration of mass to velocities above 1600 m/sec and the manipulation of materials at temperatures above 3000° K.

Although many other interesting applications of magneto- and electrofluidmechanics exist at lower temperatures (e.g., pumping of liquid metals) all these other applications are technologically less demanding by comparison.

There is not much doubt that this is a very broad field of study indeed, since it involves all of classical physics and thermodynamics (through the coupling of the Maxwell equations with the laws of motion and conservation), most of modern physics (e.g., through the equation of state and atomic and molecular ionization, excitation, and radiative processes) and most of chemistry (e.g., through the law of mass action). In fact few fields, if any, hold

* This work was sponsored in part by the U.S. Air Force Office of Scientific Research under contracts F49620-83-C-0115 and F49620-84-C-0068 under the direction of Majors Henry Pugh and Bruce Smith. Their unflinching support under adverse conditions is gratefully acknowledged.

more promise for solving some of the outstanding engineering problems of mankind. Great opportunities exist in this field of study connected with such fields of endeavor as education, research, and development, the modernization of industry, energy self-sufficiency, and others.

Needless to say, the degree of complexity of this field of study is commensurate with the number of disciplines involved and in fact the pace of success in it is intimately coupled to and exposes all the weaknesses of these disciplines. Without careful planning there is constant danger that the weakest link of the weakest scientific or engineering disciplines involved will dictate the pace of development of this field.

The United States government alone has spent in excess of $500 million in the last ten or twenty years attempting to reduce to practice or commercialize various applications of magneto- and electrofluid mechanics. The magnitude of the problems and the original misunderstanding exhibited by many investigators engaged in these fields were such that not much has yet materialized from all these efforts.

2. FUNDAMENTAL THEORY

2.1 The Equations of Charged and Conducting Fluids

Magnetofluidmechanics is concerned with the mechanics of fluids which may support electromagnetic body forces. These forces arise from the presence in the fluid of a charge density ρ_c and a current density $\mathbf{J}_0$. The total current density $\mathbf{J}_0$ consists of a convected portion $\rho_c\mathbf{U}$ and a conduction portion $\mathbf{J}$ which is carried by charge drifting at a relative velocity with respect to the macroscopic mean velocity $\mathbf{U}$. The electromagnetic force density which acts upon the fluid is given by

$$\mathbf{f} = \rho_c\mathbf{E} + \mathbf{J}_0 \times \mathbf{B} \tag{2.1}$$

where $\mathbf{E}$ and $\mathbf{B}$ are the electric and magnetic fields which are themselves determined by the charge and current present both in the fluid and its surroundings. The corresponding power flow from the electromagnetic field to the fluid is given by

$$P = \mathbf{J}_0 \cdot \mathbf{E}. \tag{2.2}$$

The macroscopic (as opposed to the species) conservation laws for a fluid subject to electromagnetic forces are

$$\frac{D\rho}{Dt} + \rho\nabla \cdot \mathbf{U} = 0, \tag{2.3a}$$

$$\rho\frac{D\mathbf{U}}{Dt} + \nabla p = \nabla \cdot \mathbf{\Pi} + \rho_c\mathbf{E} + \mathbf{J}_0 \times \mathbf{B}, \tag{2.3b}$$

$$\rho\frac{D}{Dt}(\epsilon + U^2/2) + \nabla\cdot(p\mathbf{U}) = \nabla\cdot(\mathbf{\Pi}\cdot\mathbf{U}) + \nabla\cdot\mathbf{q} + \mathbf{J}_0\cdot\mathbf{E}. \qquad (2.3c)$$

The mass density, velocity, and thermal energy per unit mass of the fluid are ρ,U, and ϵ. The pressure is p, $\mathbf{\Pi}$ is the viscous stress tensor, and $\mathbf{q}$ the heat flux vector.

Since each species (electrons, ions of different charge, atoms or molecules of different mass) in the fluid may have its own temperature, number density, etc. and its own constitutive or transport properties, Eqs. (2.3) are more properly written separately for each species and then appropriately summed. However, that treatment is beyond the scope of this article. It can be found in such sources as Demetriades et al. 1963, 1966, 1982 and Argyropoulos et al., 1969, and Sutton and Sherman, 1964).

In most engineering applications of MHD there are important regions where the electron temperature is not the same as the gas temperature and the electron number density does not correspond to the gas temperature through some appropriate Saha equation (at the gas temperature) but is closer or equal to the number density obtained from a Saha equation at the electron temperature (Kerrebrock, 1962.) it is important to retain in the system of Eqs. (2.3) at least the separate electron energy equation which couples the local electron temperature to the electric and magnetic fields and local electron number density.

An adequate form of this electron energy equation is

$$\mathbf{J}_e\cdot\mathbf{E}' = 3/2kn_e\nu\delta_{eff}(T_e - T_a) + \dot{R} + \sum_i \dot{s}_1\epsilon_i \qquad (2.3d)$$

where $\mathbf{J}_e$ is the electron current, $\dot{R}$ represents the radiative losses from the electrons, $\dot{s}_i$ is the rate of "chemical" reaction of electrons and heavy particles per unit volume per unit time, ϵ_i is the characteristic energy that is exchanged in each such reaction i in units of energy per reaction, k is the Boltzmann constant, n_e is the number density of electrons, ν is the total electron collision frequency, δ_{eff} is the effective energy loss factor per electron collision that involves elastic and inelastic energy exchange, T_e is the electron temperature, T_a is the heavy species (atoms, molecules or ions) temperature, and m_e is the mass of the electron. Usually, for diatomic or polyatomic gases and at temperatures of current interest in MHD, $\dot{R}$ and $\dot{s}_i$ are negligible compared to the collision term that contains $(T_e - T_a)$.

The conservation laws Eqs. (2.3) must be supplemented with thermodynamic state equations

$$n_\alpha = n_\alpha(p,T), \qquad p = p(\rho,T), \qquad e = e(\rho,T). \qquad (2.4)$$

The n_α are the number densities of the various species which compose the plasma. A preeminent species in an ionized gas is the electron number density n_e whose equlibrium state equation (2.4) is known as the Saha equation. For a singly ionizable species of number density n_s, the Saha equation has the simple form

$$\frac{n_e^2}{n_s} = \frac{2\pi m_e kT_e}{h^2}e^{-\epsilon/kT_e}.$$

where h is Planck's constant and ϵ is the ionization energy. Although we have indicated no dependence upon the electromagnetic fields in the state relationships, it should be noted that fluids with permanent electric or magnetic dipoles possess thermodynamic property functions which depend explicitly upon the fields **E**, **B** (de Groot and Mazur, 1962; Penfield and Haus, 1967).

The constitutive relationships for the stress, heat flux, and conduction current consistent with the Navier-Stokes level of approximation are

$$(\mathbf{\Pi})_{ij} = -2\rho\nu\left[\frac{1}{2}\left(\frac{\partial U_i}{\partial x_j}+\frac{\partial U_j}{\partial x_i}\right)-\frac{1}{3}\frac{\partial U_k}{\partial x_k}\delta_{ij}\right] \tag{2.5a}$$

$$\mathbf{q} = -\lambda\nabla T + \psi\mathbf{J}, \tag{2.5b}$$

$$\mathbf{J} = \sigma(\mathbf{E}+\mathbf{U}\times\mathbf{B}) + \phi\nabla T. \tag{2.5c}$$

Equation (2.5c) for the current **J** which complements the Navier Stokes relationship for $\mathbf{\Pi}$ and **q** in a conducting fluid is called the "Ohm's Law." The coefficients $\mu, \lambda, \sigma, \psi, \phi$ are the scalar transport coefficients of viscosity, heat conduction, and electrical conductivity. In general the heat flow and conduction current are coupled; however the coupled heat flux term $\phi\nabla T$ in the current equation may be neglected whenever the electric field $\mathbf{E}' = \mathbf{E}+\mathbf{U}\times\mathbf{B}$ is much greater in magnitude than $(k/e)\nabla T$ where k/e is the ratio of the Boltzmann constant to the electron charge.

When a magnetic field is present, the transport properties become tensorial. This effect is known as the Hall effect and is described by the Hall vector $\beta = (e/m)\mathbf{B}/\nu$ where e/m is the charge to mass ratio of the conduction carriers and ν is their effective collision frequency for momentum scattering. When $\beta \gg 1$, terms proportional to $\nabla\mathbf{U}\times\beta$, $\nabla T\times\beta$, and $\mathbf{E}\times\beta$ must appear in Eqs. (2.5a) through (2.5c) respectively. The Hall effect on the viscous stresses is of significance in fully ionized plasma in very strong magnetic fields (Braginskii,1958: Longmire and Rosenbluth, 1956). In partially ionized gases the Hall effect upon the stress tensor is generally negligible although its influence upon the heat flux and current may be substantial. In partially ionized gases the principal contribution to the stress tensor arises from the collisional interaction of the heavy species in the gas, most of which are not charged.

The full "generalized Ohm's Law" including the case when the electron temperature is not equal to the heavy species temperatures has been developed (Demetriades, Hamilton, Ziemer, and Lenn, 1962; Demetriades and Argyropoulos, 1966; Schweitzer and Mitchner, 1967). In the simplest case in which temperature gradients may be neglected, Eq. (2.5c) becomes

$$\mathbf{J}_\perp = \frac{\sigma}{(1+\beta^2)}(\mathbf{E}_\perp - \mathbf{E}_\perp\times\beta), \tag{2.7a}$$

$$\mathbf{J}_\parallel = \sigma\mathbf{E}_\parallel, \tag{2.7b}$$

where $\perp$ and $\parallel$ denote directions perpendicular and parallel to the magnetic field respectively. The electric field $\mathbf{E}' = \mathbf{E} + \mathbf{U} \times \mathbf{B}$ is the electric field in a frame of reference moving with the fluid velocity $\mathbf{U}$. Using Eqs. (2.7) the expression $\mathbf{J} \cdot \mathbf{E}'$ may be expressed as

$$\mathbf{J} \cdot \mathbf{E}' = J^2/\sigma = \frac{\sigma}{(1+\beta^2)}(E'_\perp)^2 + \sigma E_\parallel^2.$$

The power flow $\mathbf{J} \cdot \mathbf{E}'$ is positive definite ("Joule dissipation") and represents the dissipation of electrical power into internal thermal energy as follows from the thermal energy equation which results from Eq. (2.3c) with the kinetic energy $U^2/2$ eliminated by Eq.(2.3b).

The charge density ρ_c and current J_0 determine the fields $\mathbf{E}, \mathbf{B}$ through the Maxwell equations:

$$1/c^2 \partial \mathbf{E}/\partial t - \nabla \times \mathbf{B} = -\mu_0 \mathbf{J_0}, \tag{2.8a}$$

$$\partial \mathbf{B}/\partial t + \nabla \times \mathbf{E} = \mathbf{0}, \tag{2.8b}$$

$$\nabla \cdot \mathbf{E} = \rho_c/\epsilon_0, \tag{2.8c}$$

$$\nabla \cdot \mathbf{B} = 0. \tag{2.8d}$$

Equations (2.3) and (2.8) with the state and constitutive relationships (2.4), (2.5), and (2.7) form a closed coupled system for the fluid variables $\rho, \mathbf{U}, \epsilon, \rho_c, \mathbf{J_0}$ and the electromagnetic field variables $\mathbf{E}$ and $\mathbf{B}$.

2.2 Theorems of Bernoulli and Kelvin

Using the identity $\mathbf{U} \cdot \nabla \mathbf{U} = \nabla U^2/2 - (\nabla \times \mathbf{U}) \times \mathbf{U}$, the momentum equation may be expressed as

$$\begin{aligned} \rho(\partial \mathbf{U}/\partial t - \mathbf{\Omega} \times \mathbf{U} + \rho \nabla U^2/2) + \nabla(p+w) \\ = -\nabla \cdot \mathbf{\Pi} + \mu_0^{-1} \mathbf{B} \cdot \nabla \mathbf{B} + \epsilon_0(\mathbf{E} \cdot \nabla \mathbf{E} - \rho_c \mathbf{E}), \end{aligned} \tag{2.9}$$

where $\mathbf{\Omega} = \nabla \times \mathbf{U}$ is the vorticity and $w = (\epsilon_0 E^2 + \mu_o^{-1} B^2)/2$ is the electromagnetic energy density. When the right hand side of Eq. (2.9) vanishes under conditions of uniform density, Bernoulli's theorem for electromagnetic flow is obtained:

$$U^2/2 + (\epsilon_0 E^2 + \mu_o^{-1} B^2)/2 + p/\rho = C(t). \tag{2.10}$$

Particular velocity fields which possess Bernoulli integrals Eq. (2.10) include all velocity fields which may be represented as $\mathbf{U} = \mathbf{k_1} \times \mathbf{E} + \mathbf{k_2} \times \mathbf{B}$ where $\mathbf{k_1}$ and $\mathbf{k_2}$ are arbitrary vectors. All electromagnetic fields which are free of tangential gradients similarly allow the existence of a Bernoulli integral. Most general flows of engineering interest do not satisfy these conditions.

The curl of Eq. (2.3b) at uniform density yields the vorticity equation in electromagnetic flow:

$$\rho(D\boldsymbol{\Omega}/Dt - \boldsymbol{\Omega}\cdot\nabla\mathbf{U}) = -\nabla\times(\nabla\cdot\boldsymbol{\Pi}) + \mathbf{B}\cdot\nabla\mathbf{J}_0 - \mathbf{J}_0\cdot\nabla\mathbf{B} + \rho_c\nabla\times\mathbf{E}. \tag{2.11}$$

When the RHS of Eq. (2.11) vanishes Kelvin's theorem is obtained: the flux of vorticity through an elemental area $\boldsymbol{\Omega}\cdot\delta\mathbf{A}$ is conserved. In conventional flow, viscous stresses act as the only mechanism for the creation of vorticity; however in electromagnetic flow, the curl of the Lorentz force does not generally vanish even in the case of "ideal" flow in which $\sigma^{-1}\to 0$ and there is no Joule dissipation. Gradients of the current density in the direction of the magnetic field can represent an important source of vorticity in electromagnetic flow.

2.3 The Magnetohydrodynamic and Electrohydrodynamic Approximations

The divergence of Eq. (2.8a) and use of Eq. (2.8c) with $\mathbf{J}_0 = \rho_c\mathbf{U} + \mathbf{J}$ yields the equation governing the charge density:

$$D\rho_c/Dt + \rho_c\nabla\cdot\mathbf{U} = -\rho_c/\epsilon_0. \tag{2.12}$$

From Eq. (2.12) τ_c, the decay time for charge, is given by $\tau_c = \epsilon_0/\sigma$. If $t = L/U$ is a characteristic macroscopic time scale where L is the length scale, the condition $t/\tau_c = (L/\tau_c U)\approx 1$ divides conductors from non-conductors. If $t/\tau_c \ll 1$, the *electrohydrodynamic approximation* $\mathbf{J}\approx 0$ holds and

$$D\rho_c/Dt + \rho_c\nabla\cdot\mathbf{U} = 0. \tag{2.13a}$$

Correspondingly the Lorentz force becomes

$$\mathbf{f} = \rho_c(\mathbf{E} + \mathbf{U}\times\mathbf{B}). \tag{2.13b}$$

For $t/\tau_c \gg 1$ there results $\rho_c\approx 0$ and $\mathbf{J}_0 = \mathbf{J}$. Equation (2.12) then becomes

$$\nabla\cdot\mathbf{J} = 0, \tag{2.14a}$$

which requires that Eq. (2.8a) takes the form

$$\nabla\times\mathbf{B} = \mu_0\mathbf{J}. \tag{2.14b}$$

Correspondingly the Lorentz force becomes

$$\mathbf{f} = \mathbf{J}\times\mathbf{B}. \tag{2.14c}$$

The approximation embodied in Eqs. (2.14) which stems from $\rho_c = 0$ is known as the ***magnetohydrodynamic approximation.*** Note particularly that the neglect of $\partial\mathbf{E}/\partial t$ from Eq. (2.8b) in this approximation prohibits a description of electromagnetic radiation.

2.4 The Equation of Magnetic Induction

The elimination of **J** and **E** from Eq. (2.14b) and the Ohm's Law with Eq. (2.8b) results in the induction equation for **B** for uniform density and electrical transport properties σ, β :

$$D\mathbf{B}/Dt - \mathbf{B} \cdot \nabla \mathbf{U} = \eta \nabla^2 \mathbf{B}. \tag{2.16}$$

Equation (2.16) describes the convection and diffusion of the magnetic field with the magnetic diffusivity $\eta = 1/\mu_0 \sigma$. When $\eta \to 0$, the electrical forces are non-dissipative and the magnetic field is convected as if the lines of force were bound to the fluid. The left hand side of Eq. (2.16) is formally identical to the vorticity equation Eq. (2.11): $\mathbf{B} \cdot \delta\mathbf{A}$, the flux of B through an elemental area $\delta\mathbf{A}$, is conserved throughout the flow just as the flux of vorticity $\mathbf{\Omega} \cdot \delta\mathbf{A}$ is conserved when Kelvin's theorem holds.

The time scale τ_B for the field to diffuse over a length scale L is found from (2.16) to be

$$\tau_B = L^2/\mu_0 \sigma. \tag{2.17}$$

The convective time scale L/U may be compared to the diffusion time scale τ_B in a non-dimensional parameter known as the magnetic Reynolds number R_m (Lundquist, 1952):

$$R_m = \tau_B/(L/U) = \mu_0 \sigma U L. \tag{2.18}$$

For $R_m \ll 1$, magnetic fields diffuse rapidly through the region of interest. The regime of vanishing R_m has other important consequences. Consider a steady magnetic field $\mathbf{B_0}$ which is established by currents external to the fluid. Let **J** be the current present in the fluid and $\mathbf{B'}$ given by Eq. (2.14b) the field induced by the currents in the fluid. From Ohm's Law with $\mathbf{E} \approx \mathbf{U} \times (\mathbf{B_0} + \mathbf{B'})$ the current is given by $\mathbf{J} \approx \sigma \mathbf{U} \times (\mathbf{B_0} + \mathbf{B'})$. The field $\mathbf{B'}$ induced by this current is from Eq. (2.14b)

$$\nabla \times \mathbf{B'} \approx \mu_0 \mathbf{J} \approx \mu_o \sigma \mathbf{U} \times (\mathbf{B_0} + \mathbf{B'}). \tag{2.19}$$

Since $|\nabla \times \mathbf{B'}| \approx B'/L$, there results

$$\frac{B'}{B_0 + B'} \approx \mu_0 \sigma U L = R_m. \tag{2.20}$$

When $R_m \geq 1$, the field satisfies $B'/B_0 \approx 1$; but for $R_m \ll 1$, this condition becomes $B'/B_0 \approx R_m \ll 1$ and the induced field $\mathbf{B'}$ may be neglected compared to the applied field $\mathbf{B_0}$. From Eq. (2.8b) we have $\partial \mathbf{B}/\partial t \approx -\nabla \times \mathbf{E}$. For $\mathbf{E} \approx \mathbf{U} \times \mathbf{B'}$ and $\partial/\partial t$ of the order of the convective time scale U/L it will be true that

$$\frac{|\partial \mathbf{B'}/\partial t|}{|\nabla \times \mathbf{E}|} \approx R_m. \tag{2.21}$$

In the approximation of low magnetic Reynolds number Ohm's Law is expressed only in terms of applied field $\mathbf{B_0}$:

$$\mathbf{J} = \frac{\sigma}{(1+\beta_0^2)}\left[\mathbf{E} + \mathbf{U}\times\mathbf{B_0} - \beta_0 \times (\mathbf{E} + \mathbf{U}\times\mathbf{B_0})\right], \tag{2.22}$$

while the Maxwell equation (2.8b) becomes

$$\nabla \times \mathbf{E} = \mathbf{0}, \tag{2.23}$$

and Eq. (2.8a) in the MHD approximation becomes

$$\nabla \cdot \mathbf{J} = 0. \tag{2.24}$$

Equations (2.22)-(2.24) serve to completely determine the fields **E**, **J** in the *low magnetic Reynolds number* and *MHD approximations*. The magnetic field $\mathbf{B} \ll \mathbf{B_0}$ induced by the current governed by Eqs. (2.22) - (2.24) may be determined from Eq. (2.14b).

2.5 Characteristic Parameters

The characteristic parameters for the general fluid equations in absence of body forces are three: The Mach number $M = U/c$ (where $c = \sqrt{\gamma p/\rho}$ is the speed of sound), the viscous Reynolds number $R_e = UL/\nu$, and the Prandtl number $P_r = C_p\nu/\rho\lambda$ where C_p is the specific heat at constant pressure. Additional parameters are required in magnetohydrodynamic flow.

The first of these parameters is the magnetic Reynolds number R_m which describes the convection of magnetic energy compared to its diffusion. One other independent one-dimensional number is required for the description of electromagnetic effects in the MHD approximation. For $R_m \gg 1$ the ratio of magnetic energy density to the fluid energy density is an appropriate choice:

$$I_U = B^2/\mu_0\rho U^2. \tag{2.25}$$

A second choice is the ratio of magnetic pressure to fluid pressure:

$$I_p = B^2/\mu_0 p. \tag{2.26}$$

The parameters I_U, I_p are not independent but are related through the Mach number M :

$$I_p = \gamma M^2 I_U. \tag{2.27}$$

Under conditions where $R_m \ll 1$, magnetic diffusion effects dominate over convection and a more appropriate choice of parameters are the interaction parameters S_U and S_p. The parameter S_U is defined as the ratio of the Lorentz force (with **J** expressed from Ohm's Law) to the change of fluid momentum in length L:

$$S_U = \sigma B^2 L/\rho U. \tag{2.28}$$

The parameter S_p is the ratio of the Lorentz force (similarly expressed through the Ohm's Law) to the pressure gradient over length L :

$$S_p = \sigma U B^2 L/\rho. \tag{2.29}$$

The parameters S_U, S_p are not independent of I_U, I_p but are related through the magnetic Reynolds number:

$$S_U = R_m I_U, \tag{2.30a}$$

$$S_p = R_m I_p. \tag{2.30b}$$

The Hartmann number H_a is defined as

$$H_a = \sqrt{S_U R_e}. \tag{2.31}$$

and is a measure of the ratio of the Lorentz force to the viscous force.

For general magnetohydrodynamic flow, a typical and complete set of independent parameters are M, R_e, P_r, R_m, and S_U. When the electrical conductivity is tensorial due to Hall effect, the Hall parameter β must be added to this set.

3. BASIC MAGNETOHYDRODYNAMIC PROCESSES

3.1 Local Currents and Fields

Consider the nature of the currents and fields **J**,**E** in a local region of flow. From the Ohm's Law Eq. (2.7) it can be seen that the magnetic field effects involve $\mathbf{U} \times \mathbf{B}$ and $(\mathbf{U} \times \mathbf{B}) \times \beta$. These effects are confined to the plane perpendicular to **B**. Orient **B** in the z direction so that $\mathbf{B} = \mathbf{B}(0, 0, B)$, **U** in the x (axial) direction with $\mathbf{U} = \mathbf{U}(U, 0, 0)$, and let $\mathbf{E} = \mathbf{E}(E_x, E_y, 0)$ where y represents the transverse direction. The axial and transverse load factors K_x, K_y which serve to summarize the nature of the external electrical connection to the conducting fluid are defined as

$$K_x = \frac{-E_x}{\beta U B(1 - K_y)}, \tag{3.1a}$$

$$K_y = E_y/UB. \tag{3.1b}$$

The Ohm's Law Eqs. (2.7) then becomes

$$J_x = (1 - K_x)(1 - K_y)\frac{\sigma}{(1 + \beta^2)}\beta U B, \tag{3.2a}$$

$$J_y = -(1 - K_y)(1 + K_x\beta^2)\frac{\sigma}{(1 + \beta^2)}UB. \tag{3.2b}$$

For $K_y = 1$ both the axial and transverse currents are "open circuited" and from Eqs. (3.1) the open circuit values of the fields are $E_x = 0$ and $E_y = UB$. For $K_x = 1$ for any K_y, the axial current vanishes and the transverse current is given by

$$J_y = -(1 - K_y)\sigma UB. \tag{3.3}$$

Thus, if J_x is prevented from flowing the transverse current J_y achieves a level equal to that which it would have in the absence of the Hall effect; an axial or "Hall" field E_x will be present, however, given by $E_x = -\beta E_y$ where $E_y = (1 - K_y)UB$. Clearly, for large Hall parameter β the axial field will dominate the transverse field. On the other hand if $K_x = 0$, the axial field is shorted and the transverse current from Eqs. (3.2) is reduced by the factor $1/(1 + \beta^2)$ from its value in the unshorted case given by Eq. (3.3).

3.2 Force, Power, and Dissipation

The local Lorentz force $\mathbf{f}(f_x, f_y, 0)$ and power P are given from Eqs. (2.1), (2.2) and (3.2) as

$$f_x = -(1 - K_y)(1 + K_x\beta^2)\frac{\sigma}{(1 + \beta^2)}UB^2, \tag{3.4a}$$

$$f_y = -(1 - K_x)(1 - K_y)\frac{\sigma}{(1 + \beta^2)}\beta UB^2, \tag{3.4b}$$

$$P = -(1 - K_y)\left[K_y(1 + K_x\beta^2) + (1 - K_y)(1 - K_x)K_x\beta^2\right]\frac{\sigma U^2B^2}{(1 + \beta^2)}. \tag{3.5a}$$

The dissipated power $P' = \mathbf{J} \cdot \mathbf{E}'$ is given by

$$P' = (1 - Ky)^2(1 + \beta^2K_x^2)\frac{\sigma U^2B^2}{(1 + \beta^2)}. \tag{3.5b}$$

For $K_x < 1, K_y < 1$ the force f_x is opposed to the flow velocity U and power ($P < 0$) is extracted from the flow. For $K_y > 1$, the force f_x is in the direction of the flow and power($P > 0$) must be supplied to the fluid by the fields. For $K_x > 0$, a transverse force f_y will exist in addition to the axial force f_x if $\beta > 0$. For strong Hall effect $\beta \gg 1$ this force will dominate the axial force f_x creating significant transverse pressure gradients and, under some circumstances, secondary flow.

The total axial force F_x and power $\mathcal{P}$ which can be developed in a volume V are given by

$$F_x = -\int_V dv(1 - K_y)\sigma UB^2, \tag{3.6}$$

$$\mathcal{P} = -\int_V dv(1 - K_y)K_y\sigma U^2B^2. \tag{3.7}$$

In a uniform system these expressions have the simple forms

$$F_x = -(1 - K_y)\sigma U B^2 V, \tag{3.8}$$

$$\mathcal{P} = -(1 - K_y)K_y\sigma U^2 B^2 V. \tag{3.9}$$

It is important to observe that Eqs. (3.8) and (3.9) follow from Eqs. (3.6) and (3.7) only in the case that K_y, σ, U, and B are uniform over the volume V. In most realistic magnetohydrodynamic flows these quantities are significantly non-uniform (Demetriades, Argyropoulos, and Kendig, 1967; Demetriades and Argyropoulos, 1969) and the total force or the total power cannot be reliably calculated from Eqs. (3.8) and (3.9).

3.3 Magnetic Meter and Pump

Consider a channel aligned in the x direction with crossed electric $\mathbf{E}(0, E_y, 0)$ and magnetic $\mathbf{B}(0, 0, B)$ fields. The steady one-dimensional incompressible flow equations in the low magnetic Reynolds number limit with f_x given by Eq. (3.4a) are

$$\frac{\partial U}{\partial x} = 0, \tag{3.10}$$

$$\frac{\partial p_0}{\partial x} = -(1 - K_y)\sigma U B^2. \tag{3.11}$$

where $p_0 = p + \rho U^2/2$ is the stagnation or total pressure. Since the condition $\nabla \times \mathbf{E} = \mathbf{0}$ holds we have $E_y = -\Phi/h$ where Φ is the voltage across the gap h. From Eq. (3.1b) this voltage is given by $\Phi = -K_y U B h$. The pressure change Δp_0 in length L of the channel is found from Eq. (3.11):

$$\Delta p_0 = -(1 - K_y)\sigma U B^2 L. \tag{3.12}$$

The total current per unit depth w which flows in length L is given by

$$I/w = J_y L = -(1 - K_y)\sigma U B^2 L. \tag{3.13}$$

The pressure change can thus be represented as

$$\Delta p_0 = (I/w)B. \tag{3.14}$$

The power delivered to the fluid per unit depth is

$$PL = J_y E_y L = -(I/w)\Phi. \tag{3.15}$$

At open circuit $I = 0$ the voltage at this condition is given by $\Phi = \Phi_{oc} = -UBh$. This voltage can, in principle, be used to meter the average velocity U which exists in the channel when a known magnetic field is applied over the gap of known dimension h. In practice such meters must be corrected for leakage current losses and polarization voltages which

exist on the electrodes for small devices. For a device of dimension $h = 10cm$ and imposed magnetic field $B = 0.1Tesla$, a velocity of $10m/s$ will register only $100mV$. Faraday attempted to measure the velocity of the Thames River using this principle. Although $h \approx 100m$ for the river, the earth's magnetic field is only of the order $10^{-4}Tesla$ and thus $\Phi_{oc} \approx 10mV$ for $U \approx 1m/s$ which is in the noise range of the spurious leakage and polarization effects.

To operate the channel as a pump ($\Delta p_0 > 0$) a voltage $\Phi < -UBh$ must be imposed across the gap. At the no-flow condition $U = 0$, the pressure rise is maximum and is given by

$$(\Delta p_0)_{max} = (-\Phi)\sigma BL/h. \tag{3.16}$$

For liquid metals, the pumping voltage is low because of the high electrical conductivity. For $L/h \approx 1$, $B \approx 1Tesla$, $\sigma \approx 10^7 S/m$, and $(\Delta p_0)_{max} \approx 1atm$. the pumping voltage Φ is of the order $\Phi \approx 1volt$. The corresponding current from Eq. (3.13) is $(I/w) \approx 10^7 A/m$ and the power per unit depth is $P_L = 100kW/m$. These voltage-current characteristics place a severe demand on the pump power supply.

4. FUNDAMENTAL MAGNETOHYDRODYNAMIC FLOWS

4.1 Quasi One-Dimensional Compressible Flow

In the quasi-one-dimensional description, the flow variables are averaged quantities over the cross- section of a duct. The conservation laws Eqs. (2.2) integrated over the cross-section with the variables now representing averages over the cross-section A are

$$\frac{\partial(\rho A)}{\partial t} + \frac{\partial(\rho U A)}{\partial x} = \Sigma_\rho, \tag{4.1a}$$

$$\frac{\partial(\rho U A)}{\partial t} + \frac{\partial(\rho U^2 A)}{\partial x} = -A(\frac{\partial p}{\partial x} - f_x) - \tau_w C + \Sigma_U, \tag{4.1b}$$

$$\frac{\partial[\rho(U^2/2 + \epsilon)A]}{\partial t} + \frac{\partial(\rho U h_0 A)}{\partial x} = PA + q_w C + \Sigma_\epsilon. \tag{4.1c}$$

The dependent fluid variables are the pressure p, enthalpy $h = e + p/\rho$, and stagnation enthalpy $h_0 = h + U^2/2$. The local duct cross-sectional area is A and the local perimeter is C. The functions Σ_ρ, Σ_U, and Σ_ϵ describe the sources of mass, momentum and energy due to mass addition (or depletion) within the flow train. In addition to the conservation laws, the caloric and kinetic equations of state (2.3) complete the description. The average wall shear stress over the cross-section is τ_w and the average heat flux is q_w. These averages are composites of the electrode wall and insulating wall shear stresses and heat fluxes. These quantities may be computed from the boundary layer equations for each wall. The

results of these boundary layer calculations may be summarized in the local, dynamic friction factor $C_f(x,c,t)$ and Stanton number $S_T(x,c,t)$ where c is a perimeter coordinate. The wall shear and heat flux are directly computed in terms of these quantities and then averaged over the cross section to obtain the average wall stress and heat flux which appear in Eqs. (4.1) (Oliver, Crouse, Maxwell and Demetriades, 1980).

The most fundamental solutions of Eqs. (4.1) which illustrate electromagnetic effects are those for steady, uniform area flow in the absence of viscous and heat conduction effects. Eqs. (4.1) are three simultaneous equations for the primitive variables ρ, U, ϵ. We may eliminate these variables in favor of one equation in the Mach number $M = U/\sqrt{\gamma p/\rho}$ using Eqs. (3.4a) and (3.5a) for f_x and P with $K_x = 1$:

$$\frac{1}{M^2}\frac{dM^2}{dx} = S'_p \frac{(\gamma-1)(1+\gamma M^2)}{\gamma(1-M^2)}[(1-K_y)(K_* - K_y)], \tag{4.2}$$

where $K_*(M)$ is defined as

$$K_*(M) = \frac{\gamma}{(\gamma-1)}\frac{1+(\gamma-1)/2M^2}{1+\gamma M^2}.$$

In Eq. (4.2), $S'_p \equiv \sigma U B^2/p$ is the pressure interaction parameter per unit length. This equation defines the conditions which drive the flow to or from the choke point $M = 1$. For all $K_y < 1$ the Lorentz force opposes the flow and drives the flow to the sonic point. For all $K_y > 1$ the Lorentz force acts in the direction of the flow and drives the flow away from the sonic point. When $(1 - K_y) \approx 1$ holds the effect of the Joule heating term is always to drive the flow to the sonic point: there are, however, values of K_y for which the bracketed term on the right hand side of Eq. (4.2) vanishes and continuous passage through $M = 1$ in an "electromagnetic throat" is, in principle, possible (Neuringer, 1963). It can be seen that there are two possible "throats" at $K_y = 1$ and $K_y = K_*(1) = \gamma/2(\gamma-1)$.

Exact integrals for steady flow in the absence of friction and heat transfer exist (Rosa, 1968, pp. 51-54). For the general case of flow which is unsteady and in which viscous and heat conduction effects are important the solutions are best obtained by finite difference methods. Such solutions of Eqs. (4.1) are presented in Section 6.

4.2 Viscous, Incompressible, Magnetohydrodynamic Flow

Equations (2.3) and (2.5a) for steady, incompressible, low R_m flow in the x direction between the planes $z = \pm h$ in the presence of $\mathbf{B} = \mathbf{B}(0,0,B)$, $\mathbf{U} = \mathbf{U}(U_x,0,0)$, $\mathbf{J} = \mathbf{J}(0,J_y,0)$ and $\mathbf{E} = \mathbf{E}(0,E_y,0)$ reduce to

$$\frac{\partial U_x}{\partial x} = 0, \tag{4.3a}$$

$$\frac{\partial p}{\partial x} = J_y B + \rho\nu\frac{\partial^2 U_x}{\partial z^2}, \tag{4.3b}$$

$$J_y = -\sigma(E_y - U_x B). \tag{4.3c}$$

Since $U_x = U_x(z)$, define K_y as $K_y = E_y/\langle U_x\rangle B$ where $\langle U_x\rangle$ is the average velocity between the planes $z = \pm h$. The Ohm's Law Eq. (4.3c) then becomes

$$J_y = -\sigma(U_x - \langle U_x\rangle K_y)B. \tag{4.4}$$

It can be seen that the current and the Lorentz force reverse at the point where $U_x = K_y\langle U_x\rangle$ with $J_y > 0$ for $U_x < K_y\langle U_x\rangle$ and $J_y < 0$ for $U_x > K_y\langle U_x\rangle$. Combining Eqs. (3.3b) and (3.4) and observing that $\partial^2 p/\partial x\partial z = 0$ since there is no motion in the transverse direction there results

$$\frac{\partial^2 U_x}{\partial z^2} - \frac{H_a^2}{h^2}\left[U_x - (K_y + S_p^{-1})\langle U_x\rangle\right] = 0, \tag{4.5}$$

where $H_a \equiv Bh\sqrt{\sigma/\rho\nu}$ is the Hartmann number and $S_p = \sigma B^2\langle U_x\rangle/(-\partial p/\partial x)$is the pressure interaction parameter.

The solution to Eq. (4.5) for $U_x(z)$ satisfying the boundary conditions $U_x(h) = U_x(-h)$ is

$$U_x(z) = (K_y + S_p^{-1})\langle U_x\rangle\left[1 - \frac{\cosh H_a z/h}{\cosh H_a}\right]. \tag{4.6}$$

By taking the average of Eq. (4.6), the interaction parameter S_p may be represented as a function of Hartmann number and load factor:

$$S_p = \frac{\sigma B^2\langle U_x\rangle}{(-\partial p/\partial x)} = \frac{H_a - \tanh H_a}{(1 - K_y)H_a + K_y \tanh H_a}. \tag{4.7}$$

Equation (4.7) may be used to determine the average velocity in terms of the Hartmann number, load factor, and the pressure gradient. For $H_a \gg 1$, we find $S_p \approx 1/(1-K_y)$ with the Lorentz force balancing the pressure gradient. For $H_a \ll 1$, we have $\tanh H_a \approx H_a - H_a^3/3$ and $S_p \approx H_a^2$ so that the pressure gradient is balanced against the viscous force. Using Eq. (4.7), the velocity profile (4.6) may be expressed edxclusively in terms of Hartmann number:

$$U_x/\langle U_x\rangle = \frac{H_a}{H_a - \tanh H_a}\left[1 - \frac{\cosh H_a z/h}{\cosh H_a}\right]. \tag{4.8}$$

The velocity profiles for insulating walls are shown in Fig. 4.1 as a function of Hartmann number. The effect of the magnetic field is to flatten the velocity profile in the core where $J_y < 0$, $f_x < 0$ and to enhance the profile near the sidewalls where $J_y > 0$ and $f_x > 0$.

5. LARGE MAGNETIC REYNOLDS NUMBER

Flow at large magnetic Reynolds number is characterized by the presence of magnetic fields induced by currents flowing in the fluid which are comparable to externally imposed magnetic fields. These internal fields, set up by the internal currents, tend to oppose the imposed field (Lenz' Law) thereby driving the total magnetic field from the conducting fluid. At large magnetic Reynolds numbers the currents and fields are confined to a thin zone at the boundaries of the conducting fluid.

5.1 Magnetic Field of a Conducting Fluid Slab

A fluid with a uniform velocity $\mathbf{U} = \mathrm{U}(U_x, 0, 0)$ moves in a channel of dimension $a \ll L$ where $L$is the scale of variation of an imposed magnetic field $\mathbf{B}_0 = \mathbf{B}_0(0, 0, B_0)$. Scalar conductivity of magnitude σ is switched on between the planes $x = 0.a$. The conductivity vanishes outside this slab.

The governing equation for $B_z(x)$ in steady flow is Eq. (2.16) (with $\beta = 0$):

$$U\frac{\partial B_z}{\partial x} = \eta\frac{\partial^2 B_z}{\partial x^2}, \tag{5.1}$$

while the current is determined from Eq. (2.14b):

$$J_y = -\mu_0\frac{\partial B_z}{\partial x}. \tag{5.2}$$

The boundary values are $B_z(a), B_z(0)$. The total current per unit depth flowing through the slab is given in terms of the boundary values by

$$I = \int_0^a J_y dx = -\mu_o^{-1}[B_z(a) - B_z(0)]. \tag{5.3}$$

This current is also given in terms of the load factor $K_y = E_y/UB_0$ from Eq. (3.3) as

$$I = -\int_0^a \sigma U B_0(B_z/B_0 - K_y)dx. \tag{5.4}$$

The boundary conditions to be applied to Eq. (5.1) is that the induced magnetic field immediately in front of the plasma must exactly oppose the corresponding induced magnetic field at the trailing edge of the plasma so as to maintain the condition $\nabla \cdot \mathbf{B} = \mathbf{0}$. This is equivalent to demanding that the average of the boundary values be equal to the imposed field B_0: $B_z(a) + B_z(0) = 2B_0$.

The solutions to Eqs. (5.1) and (5.2) subject to these conditions (Demetriades st. al., 1985) are

$$B_z = B_0 K_y + \frac{2B_0(1 - K_y)}{(1 + e^{R_m})}e^{R_m x/a}, \tag{5.5}$$

and

$$J_y = -\frac{2B_0\sigma U_x(1-K_y)e^{R_m x/a}}{(1+e^{R_m})}, \tag{5.6}$$

where $R_m = \mu_0 U\sigma a$ is the magnetic Reynolds number. From Eqs. (5.5) and (5.6) it can be seen that the field and current are progressively confined to a thin zone at the front of the conducting slab as the magnetic Reynolds number is increased (Fig. 5.1). The total power extracted from the conducting slab per unit of cross-section flow area A may be expressed as

$$P/A = \int_0^a J_y E_y dx = -4K_y(1-K_y)(B_0^2/2)\mu_0)U\tanh(R_m/2). \tag{5.7}$$

As the magnetic Reynolds number is increased we have $\tanh(R_m/2) \rightarrow 1$ and the extracted power is limited to the product of the magnetic energy of the applied field B_0 and the flow velocity U.

5.2 Planar Flow in an Inhomogeneous Magnetic Field

The behavior of the fields and currents in flow through an imposed localized magnetic field at large magnetic Reynolds number is inherently multi- dimensional. The imposed field $\mathbf{B_0} = \mathbf{B_0}(0,0,B_0)$ may be represented as

$$B_0(x) = B_* f(x), \tag{5.7}$$

where B_* is a constant amplitude and $f(x)$ is a shape function with a maximum at $f(0)$. The fluid is contained within the planes $y = \pm h$ and flows steadily at a uniform velocity $\mathbf{U} = \mathbf{U}(U_x,0,0)$. Conductors are arranged on the planes $y = \pm h$ over the region $|x| \leq a$. The region $|x| > a$ is an insulating surface.

The governing equation for $B_z(x,y)$ is the two- dimensional form of Eqs. (2.16):

$$U_x\frac{\partial B_z}{\partial x} = \eta\left(\frac{\partial^2 B_z}{\partial x^2} + \frac{\partial^2 B_z}{\partial y^2}\right), \tag{5.8}$$

and the current $\mathbf{J} = \mathbf{J}(J_x, J_y, 0)$ is given by

$$J_x = \mu_0^{-1}\frac{\partial B_z}{\partial y}, \qquad J_y = -\mu_0^{-1}\frac{\partial B_z}{\partial x}. \tag{5.9}$$

The boundary conditions are that the current vanish at $x = \pm\infty$ and hence $\partial B_z/\partial x = 0$ at $x = \pm\infty$. On the conductors the tangential field $E_z = J_z/\sigma$ must vanish while the normal current J_y must vanish on the insulating surfaces, i.e., $\partial B_z/\partial y = 0$.

Because of the nonuniform shape $f(x)$ and the mixed boundary conditions on $y = \pm h$ the solutions of Eqs. (5.7)-(5.10) are obtained using finite-difference methods (Oliver, Swean, and Markham, 1981). The appropriate non-dimensional parameters are the magnetic Reynolds number $R_m = \mu_0\sigma U a$ and the current load parameter $\mu_0 I/wB_*$ where the total current per unit depth flowing through the conductors to the external circuit is I/w.

In Fig. 5.2 the open circuit and loaded condition for a magnetic Reynolds number $R_m = 1$ are exhibited. It can be seen that there is an onset of eddy current cells induced in the regions of gradients in the imposed magnetic field and a convection of the current pattern downstream of the conductors. The principal current flowing in the conductors, however, is still confined to the region between the electrodes.

In Fig. 5.3 the same situation is represented but for a magnetic Reynolds number $R_m = 7$. Considerable current flow induced by the magnetic field gradients exists under open circuit conditions. Note how the upstream eddy cell couples into the electrodes. Under load, the current exists *completely downstream* from the electrodes

6. MAGNETOHYDRODYNAMIC POWER GENERATORS

Magnetohydrodynamic power generators are compact, high energy density converters of thermal energy to electricity. Such generators may function as "electro magnetic turbines" in a complete power system cycle with either a fossil or nuclear heat source and a steam bottoming plant. In this function they serve as high temperature turbines capable of handling a top cycle temperature in excess of $2500°K$ as well as slag-laden working fluid in the case of coal fired plants. Overall MHD topped plant efficiencies should be in the range of $50 - 60\%$ with the MHD generator extracting $20 - 25\%$ of the input chemical energy (Heywood and Womack, 1969). MHD generators may also function as portable devices with a rocket type combustor for short bursts of power (Maxwell and Demetriades, 1986; Velikhov, 1975); or they may be inherently unsteady driven by high energy explosives (Bangerter, Hopkins, and Brogan, 1975).

6.1 Ideal Generators

The fundamental starting point of low magnetic Reynolds number generator designs are the expressions for force and power in a basic crossed-field situation, Eqs. (3.4) and (3.5). Three principal generator types follow from these expressions: Faraday, Hall, and Diagonal. In the Faraday generator (Fig. 6.1a) the electrode walls must be segmented and multiple loads attached to preserve the condition of vanishing Hall current ($J_x = 0$, $K_x = 1$). The load current in axial length L is given by $I = J_y L w$ and the voltage across the electrodes of separation h by $\Phi = -E_y h$. This configuration possesses only an axial Lorentz force and has a power density which is not degraded by the Hall effect. The large number of load circuits are a disadvantage in this configuration. In the Hall generator (Fig. 5.1b) the Faraday circuits are shorted ($K_y = 0$) and the ends of the machine are connected to a single load. The load current for a machine of length L and transverse area hw becomes $I = J_x h w$ and the load voltage for this configuration is $\Phi = -E_x L$. This machine is only efficient at large Hall parameter β; in addition, a large transverse Lorentz force f_y exists which exceeds the axial Lorentz force and develops secondary flows and transverse pressure gradients which degrade performance.

The diagonal generator is constructed much like a Faraday generator. From Eqs. (3.1) the angle α which the equipotential lines make which are orthogonal to field lines is given by

$$\tan\alpha = -\frac{E_y}{E_x} = \frac{K_y}{\beta(1-K_y)K_x}. \tag{6.1}$$

For a given Hall parameter and operating load condition K_y, K_x the equipotentials which are orthogonal to the field lines given by Eq. (6.1) may be made of conductors and the power again extracted by a single load attached to the diagonal electrodes. This machine has the single load advantage of the Hall machine without its performance degradation. In this case the load current into a diagonal conductor is given by $I = hw(J_x - \tan\alpha J_y)$ and the load voltage by $\Phi = -E_x L$.

The local electrical efficiency η is defined as the ratio of the electrical power P to the mechanical power flow $\mathbf{f}\cdot\mathbf{U}$. The force, power, and efficiency of these configurations are given in Fig. 6.2. It will be noted that the diagonal configuration becomes inefficient at operating conditions away from its design point.

The maximum output power density for these machines is $\sigma U^2 B^2/4$. For fossil fuel combustion products seeded with an easily ionized substance such as a potassium or cesium salt, the achievable conductivity is of the order of $10 S/m$, the velocity of order $10^3 m/s$, and the magnetic field of order $10 Tesla$. The corresponding power produced by $1m^3$ of fluid is of the order $10^3 MW$.

6.2 The Magnetohydrodynamics of Real Generators

The magnetohydrodynamic flow in real generators is considerably more complex than the simple flows described in Parts 4 and 5. MHD generators are principally configured in linear ducts in which a flow proceeds along the axis of the duct of general and variable cross sectional shape and size. The Mach numbers of interest are high subsonic or moderately supersonic. The MHD interaction parameter S_U will be of the order $6-10$ for commercial scale ($300MW_{th} - 2000MW_{th}$) systems. The typical duct aspect ratio will be of the order $L/D \approx 10$. The viscous Reynolds number will be of the order $R_e = 10^6$ for typical $1m$ scale cross sections; the flow will therefore be turbulent in viscous regions. The turbulent MHD flow in such ducts will exhibit a variety of complex multi-dimensional fluid and electrical phenomena which are indicated in Fig. 6.3.

6.2.1 Thermochemistry and Electrical Conductivity

The single most important parameter for a combustion driven generator is the electrical conductivity achievable in the products of combustion seeded with an alkali salt of potassium or cesium. This quantity (as well as the full set of thermodynamic and transport properties of such gas mixtures) is well predicted by detailed thermochemical calculations (Maxwell, et. al.,1973). The inputs to these calcualtions consist of the heats of formation of all the compounds considered in the mixture, the ionization potentials of the various

ions (including electron afinities for negative ions), and the various inter-particle scattering cross sections.

The Mollier Diagram generated by these detailed thermochemical calculations for typical coal combustion products is shown in Fig 6.3 and the corresponding electrical conductivity is shown in Fig 6.4. It can be seen that over the typical expansion envelope through the generator, the electrical conductivity ranges from $10 S/m$ to $1 S/m$.

6.2.2 Boundary Layers

The fluid in the anode wall layer is subjected to a decelerating axial Lorentz force which is comparable to that in the core. It is also subjected to a transverse Lorentz force which is set up by the Hall current induced by conductivity non-uniformities between the boundary layer and the core. This force (and induced Hall current) exist even in a Faraday connection. The forces on the fluid in the anode boundary layer thus tend to lift the fluid off the wall and to induce a transverse pressure gradient. This transverse body force creates an anode boundary layer which grows in thickness faster than a conventional layer, has a weaker turbulence production within it, a larger boundary layer shape factor, and a greater tendency to stall. Such boundary layers, computed with the multi- dimensional equations (2.3) and an appropriate turbulence theory (Demetriades, Argyropoulos and Lackner, 1971) are shown in Figs. 6.6-6.8 for a generator duct flow with an interaction parameter S_U of approximately 10.

Like the anode wall, the cathode wall layer is subjected to a decelerating Lorentz force which is comparable to that in the core. The nonuniformity induced transverse force, however, is in the direction to drive the cathode wall layer fluid into the wall. A corresponding transverse pressure gradient exists as shown in Fig. 6.6. Contrary to the anode wall layer, the transverse body force on the cathode layer intensifies the turbulence production within the layer, producing a thinner boundary layer with a lower shape factor and a diminished tendency to stall compared to a conventional boundary layer. These general features of the cathode boundary layer for an $S_U \approx 10$ scale machine may be seen in Fig. 6.8.

The decelerating Lorentz force which the fluid in the sidewall boundary layer experiences is significantly diminished compared to that in the core. In a uniform conductivity flow, the velocity profiles in the boundary regions are enhanced by the Lorentz force (Hartmann effect) as described in Section 4.3. When conductivity nonuniformities are considered, the Hartmann effect becomes more pronounced and under circumstances of strong interaction ($S_U > 1$) the boundary layers possess velocity overshoots. As a result, the sidewall boundary layers run against an accelerating pressure gradient compared to the core leading to the development of velocity overshoots and negative displacement thicknesses (Fig. 6.7). The turbulence production in the part of the boundary layer below the maximum velocity point is greatly intensified over that in the anode and cathode layers due to the enhanced shearing rate of the overshot velocity profile. The skin friction and heat transfer are greatly enhanced on the sidewalls (Fig. 6.8). The sidewall layers are also free of Lorentz forces in the direct normal to their surfaces since this is the magnetic field

direction. The nature of the sidewall boundary layers in a $300MW_{th}$ machine can be seen in Fig. 6.7. Boundary layer profiles of this nature have been measured by Daily, Kruger, Self, and Eustis (1976).

In a conducting sidewall generator, the current is no longer constrained to enter the electrode across the magnetic field lines. Under some circumstances it is therefore possible for the electrode wall boundary layers to be relieved by their Lorentz forces as the current vector aligns itself with the magnetic field in the boundary layer region ($\mathbf{J} \times \mathbf{B} = 0$). In such a situation the electrode wall layers are free to experience the analogous acceleration which the sidewalls experience in an insulating wall generator and to even develop velocity overshoots, correspondingly enhanced turbulence production, shearing rate, and enhanced heat transfer rates (Markham, Maxwell, Demetriades, and Oliver, 1977.)

The actual structure of the flow in such cases will be complex because zones of enhanced Lorentz force will develop just outside the boundary layer edge as the current density intensifies but still contains a significant component in the transverse direction. Further, secondary flows which transport high momentum fluid between the sidewalls, core, and electrode walls can be expected to modify the final balance of momentum in the boundary layer regions. High-interaction conducting sidewall machines therefore require the most careful analysis of multidimensional and secondary flow effects.

6.2.3 Secondary Flow and Magnetoaerothermal Instability

It was shown in Eq. (2.11) that gradients of the current density in the magnetic field direction are a source of vorticity. When such current gradients arise purely from velocity gradients at uniform conductivity, the vorticity production is negative, i.e., the vorticity is damped (Heywood, 1963). On the other hand, when the current gradient is induced by an electrical conductivity gradient, the vorticity production is positive. Such nonuniformity induced gradients are of the essence of MHD induced secondary flow. Because of the low conductivity region near the electrodes, a Hall current J_x is induced over the electrodes (Demetriades, Argyropoulos and Casteel, 1970). This Hall current varies in the magnetic field direction due to the sidewall cooling. The resulting current density gradient becomes a source of axial vorticity. The feedback of this vorticity on the conductivity distribution can lead to amplification and an instability known as the ***magnetothermal instability*** (Demetrides, Oliver, Swean and Maxwell, 1981).

A three-dimensional evolving flow which is magnetoaerothermally unstable is shown in Figs 6.9 and 6.10. The case considered is for a subsonic segmented Faraday generator with a maximum magnetic field strength of $6Tesla$ and an interaction parameter $S_U = 10$. In Fig. 6.9 the streamlines of the vortical component of the secondary flow velocity field are shown. It should be particularly noted that even after only $1m$ of development, MHD forces have already dramatically altered the conventional turbulently generated corner secondary flow cells transforming them to fill the full cross section of the channel. In Fig. 6.10 the inherently magnetohydrodynamic character of the flow is evident in all its characteristics including the secondary flow effects. In particular, the growing, intensifying current concentration in the central anode region is prominent. This magnetoaerothermal

current concentration has brought about an extreme deceleration of the primary flow in this region and has correspondingly dramatically reduced the local skin friction in the central anode region and increased the local shape factor driving this region of the anode boundary layer towards separation (Maxwell, Swean, Vetter, Crouse, Oliver, Bangerter and Demetriades, 1981).

The anode-sidewall corner cells have evolved such that there is one large slowly rotating cell which tends to convect hot fluid into the anode and relatively colder fluid onto the cathode and a smaller more rapidly rotating cell which acts across the anode. In the cathode-sidewall corner there is a large rapidly rotating cell which acts along the sidewall boundary layer region and a similar but smaller cell which acts over part of the cathode boundary layer region. Together these cells are very efficient in bringing higher temperature fluid from the edge of the boundary layer into the corner region.

Joule heating participates with secondary flow convection in determining the temperature field. The locally enhanced temperature and conductivity produce regions of higher current densities which in turn further heat the fluid through Joule heating. This is the result of intensified Joule dissipation in certain regions which is not convected away by the secondary flows or transferred to the walls by turbulent heat conduction. Typical temperature distributions in such a situation are shown in Fig. 6.10b.

6.2.4 Time Dependent Phenomena

Time dependent phenomena in a magnetohydrodynamic flow train, Fig. 6.11, may be examined with the quasi- one-dimensional system of Eqs. (4.1) (Oliver, Crouse, Maxwell and Demetriades, 1980).A basic time dependent event is the start-up transient. This dynamic is exhibited in the space-time- amplitude plane (Fig. 6.12) including the ignition in the combustor and the injection of the ionizable potassium carbonate which takes place approximately 8 milliseconds after ignition. In Fig. 6.13, the time dependent start-up of the flow train after a steady oxidizer cold flow has been established is shown.

Of particular interest are the extreme excursions of the electric fields during this start-up transient. The axial field E_x experiences a severe overshoot (Fig. 6.14) because the velocity in the channel is high before the seed comes on and the Lorentz force decelerates the flow to its design level.

7. MAGNETOHYDRODYNAMIC ACCELERATORS

7.1 Steady Linear Accelerators

If power is supplied to the flow and $K_y > 1$ as described in Section 3.2, the Lorentz force is in the direction of flow in an MHD channel and the working fluid is accelerated. Steady flow channel solutions for the exit state of the fluid in terms of the inlet state and the applied power may be obtained analogous to those for MHD power generators (Jahn,

1968). The velocity enhancement U_e/U_0 (where U_e is the exit velocity of the channel and U_0 is the inlet velocity) is a function of the interaction parameter $S_U = \sigma B^2 L/\rho U$:

$$U_e/U_0 = \left[1 + a\langle\frac{\sigma B^2}{\rho U}\rangle L\right]^{\alpha}, \tag{7.1}$$

where $\langle\ \rangle$ indicates an average over the channel and the pure numbers a, α have different order unity values depending upon the particular assumptions of channel operation (isothermal, constant field, constant current, etc.) A pioneering steady flow accelerator, the Northrup Mk III, achieved a thrust level of approximately $45 Newtons$ at a mass flow of $1.3 g/s$ of argon and peak current densities of approximately $100 A/cm^2$ (Demetriades et. al., 1963). A member of this family of accelerators, the Mk CA-1, designed for accelerating air, is ilustrated in Fig 7.1.

7.2 The Magnetoplasmadynamic Accelerator

An accelerator of considerable interest is obtained by considering a steady flow accelerator of the type described in Section 7.1 in cylindrical coordinates with azimuthal symmetry (Fig. 7.2). For this configuration of anode and cathode in (r, θ, z) coordinates we have $\mathbf{J} = \mathbf{J}(J_r, 0, 0)$ and $\mathbf{B} = \mathbf{B}(0, B_\theta, 0)$. A current I is applied between the anode and the cathode and the Hall current is suppressed. The magnetic field may be either applied or induced by the self-current ($R_m \geq 1$) or both. With only variation in the r direction the current density is given in terms of the applied current by

$$J_r(r) = \frac{I}{2\pi r L}. \tag{7.2}$$

The induced field B_θ is determined from Eq. (2.14b):

$$\frac{\partial B_\theta}{\partial z} = -\mu_0 J_r, \tag{7.3}$$

and thus the induced magentic field is given by

$$B_\theta = -\frac{\mu_0 I}{2\pi r}(1 - z/L). \tag{7.4}$$

The Lorentz force from Eqs. (2.14c) and (2.14d) is given by $\mathbf{f} = \mathbf{f}(0, 0, f_z)$:

$$f_z = J_r B_\theta. \tag{7.5}$$

The total electromagnetic thrust force acting over the volume defined by $0 \leq z \leq L, r_c \leq r \leq r_a$ is

$$F_z = \int_0^L \int_0^{2\pi} \int_{r_c}^{r_a} f_z 2\pi r dr d\theta dz = \frac{\mu_0 I^2}{4\pi} \ln(r_a/r_c). \tag{7.6}$$

The thrust force is thus quadratic in the applied current. For typical dimensions $r_c \approx 1cm$, $r_a \approx 10cm$, and $I \approx 1kAmp$, a thrust force of the order $1/4Newton$ is generated. In general, the current pattern will possess a component in the z direction, particularly if the anode is placed downstream of the cathode. The Lorentz force component due to the presence of J_z is $f_r = -J_z B_\theta$ and represents a focusing (or inward pinching) of the jet. When the Hall effect is present, the aximuthal symmetry requires that the Hall field E_θ be shorted and a Hall current will flow given by $J_\theta \approx \beta J_r$. Correspondingly, components B_r, B_z of the magnetic field will be induced which will modify the focusing and thrust forces and also lead to a torque $r f_\theta = r(J_z B_r - J_r B_z)$ which will impart angular momentum to the fluid.

The MPD accelerator achieves a conducting fluid by the self-heating of the working fluid by the discharge itself. This machine operates most stably at low pressure; and in this regime plasma kinetic effects such as ionization and recombination, charge exchange, and strongly non-Maxwellian behavior play an important role.

REFERENCES

Argyropoulos, G.S., S.T. Demetriades and K. Lackner, 1968, "Compressible Turbulent Magnetohydrodynamic Boundary Layers," *Phys. Fluids.* vol. 11, no.12

Argyropoulos, G.S., S.T. Demetriades and A.P. Kendig, 1967, "Current Distribution in Non-Equilibrium JxB Devices," *J. Appl. Phys.* vol. 38, no.13, pp. 5233-5239

Argyropoulos, G.S. and S.T. Demetriades, 1969 "Influence of Relaxation Effects in Non-Equilibrium JxB Devices," *J. Appl. Phys.*, vol. 40, no.11, pp. 4408-4409

Argyropoulos, G.S., M.A. Casteel and S.T. Demetriades, 1970, "Two-Dimensional Distribution of Current Along Magnetohydrodynamic Channels," *Energy Conversion.* vol. 10, pp. 189-192

Bangerter, C.D., B.D. Hopkins and T.R. Brogan, 1975, "Explosively Driven MHD Power Generation - A Progress Report," *Proc. 6th Int'l Symp. on MHD Power Generation.* vol. IV, p. 155, Washington, D.C.

Braginskii, S.I., 1958 *Soviet Phys. JETP*, vol. 6, p 358

Daily, J.M., C.H. Kruger, S.A. Self, and R.A. Eustis, 1976, "Boundary-Layer Profile Measurements in a Combustion Driven MHD Generator," *AIAA J.* vol. 14, pp. 997-1005, August 1976

DeGroot, S.R. and P. Mazur, 1962, *Non-equilibrium Thermodynamics*, North Holland Publishing Company, Amsterdam and Interscience Publishers, Inc. NY

Demetriades, S.T, Hamilton, R. Ziemer and P.D. Lenn, 1963, "Three-Fluid Non-Equilibrium

Plasma Accelerators, Part I," *Progress in Astronautics and Aeronautics*, vol.9, AIAA Series, pp. 461-611, Academic Press, NY

Demetriades, S.T and G.S. Argyropoulos, 1966, "Ohm's Law in Multicomponent Non-Isothermal Plasmas with Temperature and Pressure Gradients," *Phys. Fluids*, vol.9, no.11, pp. 2136-2149

Demetriades, S.T., 1968, "Novel Method for Determination of Energy-loss Factors for Slow Electrons in Hot Gases," *STD Research Corp. Rpt. No. STD-68-2*

Demetriades, S.T. and C.D. Maxwell, 1969, "Determination of Energy-Loss Factors for Slow Electrons in Hot Gases," *STD Research Corp. Rpt. STD-69-1*

Demetriades, S.T., D.A. Oliver, T.F. Swean, Jr., and C.D. Maxwell, 1981, "On the Magnetoaerothermal Instability," Paper No. AIAA-81-0248 presented at *AIAA 19th Aerospace Sciences meeting*, St. Louis MO

Demetriades, S.T., D.A. Oliver and C.D. Maxwell, 1982, "Brief Technical Discussion of the Consistent STD/MHD Code System: Presenting the Foundation, Forumulations, Assumptions and Constitutive Building Blocks of the STD/MHD Code System," STD Research Corp. Rpt. No. STDR-82-7

Demetriades, S.T., J.T. Demetriades, and A.S. Demetriades, 1985, "Influence of Magnetic Reynolds Number on Power Generated by an Ideal MHD Device," *AIAA J.*, vol. 23, No 11, pp 1813-1814

Heywood, J.B., 1968, "The Effect of Swirl on MHD Generator Performance," *Adv. Energy Conversion*

Heywood, J.B. and G.J. Womack, 1969, *Open Cycle MHD Power Generation*, Chapter 11, Pergamon Press, London

Jahn, R.G., 1968, *Physics of Electric Propulsion*, McGraw-Hill Book Company, NY

Kerrebrock, J.L., 1962, "Conduction in Gases with Elevated Electron Temperatures," *Engineering Aspects of Magnetohydrodynamics*, Columbia Univ. Press, NY, pp. 327-346

Longmire, C. and M. Rosenbluth, 1956, *Phys. Rev.*, vol 103, p 507

Lundquist, S., 1952, "Studies in Magnetohydrodynamics," *Ark. f. Fys.* vol. 5, p. 297

Markham, D.M., C.D. Maxwell, S.T. Demetriades and D.A. Oliver, 1977, "A Numerical Solution to the Unsteady, Quasi-Three-Dimensional, Turbulent Heat Transfer Problem in an MHD Channel," Paper No. 77-HT-90 presented at *AIChE-ASME Heat Transfer Conf.*, Salt Lake City UT

Maxwell, C.D., S.T. Demetriades, G.S. Argyropoulos, N.J. Patel, and M. Easterling, 1973, "Input Data for Computation of Thermodynamic and Electrical Properties of Coal Combustion Products," *Proc. 13th Symp. on Engrg. Aspects of MHD*, Stanford CA, p VII.5.1

Maxwell, C.D., T.F. Swean, Jr. A.A. Vetter, R.D. Crouse, D.A. Oliver, C.D. Bangerter, and S.T. Demetriades, 1981, "Three-Dimensional Effects in Large Scale MHD Generators," Paper No. AIAA-81- 1231 presented at *AIAA 14th Fluid and Plasma Dynamics Conf.*, Palo Alto, CA

Maxwell, C.D. and S.T. Demetriades, 1986, "Initial Tests of a Lightweight, Self-Excited MHD Power Generator," *AIAA J.*,vol. 7, No 1, p474

Oliver, D.A., R.D. Crouse, C.D. Maxwell and S.T. Demetriades, 1980, 'Transient Processes in Large Magnetohydrodynamic Generator Flowtrains," *Proc., 7th Int'l. Conf. on Magnetohydrodynamic Electrical Power Generation*, MIT

Oliver, D.A., T.F. Swean, Jr., D.M. Markham, C.D. Maxwell, and S.T. Demetriades, 1981, "High Magnetic Reqynolds Number and Strong Interaction Phenomena in MHD Channei Flows," *Proc 7th Intl. Conf. on MHD Electrical Power Generation*, MIT

Neuringer, J.L., 1960, "Optimum Power Generation Using a Plasma as the Working Fluid," *J. Fluid Mech.*, vol.7, p. 287

Penfield, Paul Jr. and Hermann A. Haus, 1964, *Electrodynamics of Moving Media, Research Monograph No. 40*, The MIT Press, Cambridge MA.

Rosa, R.J., 1968, *Magnetohydrodynamic Energy Conversion*, McGraw-Hill Book Co., NY

Schweitzer, S. and M. Mitchner, 1967, "Electrical Conductivity of Partially Ionized Gases in a Magnetic Field," *Phys. Fluids*, vol.10, no.4, p. 799

Sutton, G.W. and A. Sherman, 1964, *Engineering Magnetohydrodynamics*, McGraw-Hill, NY, Chapter 5

Velikhov, E.P., Y. M. Volkov, A.V. Zotov, O.G. Matveeko, and A.A. Yakushev, 1975, "Investigation of Factors Affecting Self-Excitation of Pulsed MHD Generators," *Proc 6th Intl. Conf. on MHD Electrical Power Generation*, Washington, D.C.

FIGURE TITLES

Fig. 4.1 Viscous magnetohydrodynamic flow velocity profiles as a function of Hartman Number H_a. Lorentz force and current reverse at the point at which $U_x = \langle U \rangle$.

Fig. 5.1 Magnetic field distribution through plasma slab moving through an imposed external magnetic field B_0 as a function of the magnetic Reynolds number $R_m = \mu_0 \sigma U a$. Note that for $R_m \geq 10$ the field (and currents) are well excluded from most of the plasma.

Fig. 5.2 Planar flow at finite magnetic Reynolds number $R_m = 1$. The induced magnetic field isolevels are shown In (a), the electrodes are at open circuit ($\mu_0 I/B_* = 0$) and in (b) the electrodes are connected to a load ($\mu_0 I/B_* = 1$).

Fig. 5.3 Planar flow at finite magnetic Reynolds number $R_m = 7$. Induced magnetic field isolevels are shown. In (a), the electrodes are at open circuit ($\mu_0 I/B_* = 0$) and in (b) the electrodes are connected to a load ($\mu_0 I/B_* = 1$).

Fig. 6.1 Magnetohydrodynamic channel configurations.

Fig. 6.1a Faraday connected linear MHD generator.

Fig. 6.1b Hall connected linear MHD Generator. Faraday circuits are shorted and power is extracted from the ends.

Fig. 6.1c Diagonal conducting wall configuration. Diagonal conducting bars are aligned with design point equipotentials and power is extracted from the ends.

Fig. 6.2 Comparison of the output characteristics of diagonal and Faraday generators.

Fig. 6.3 Mollier diagram for a typical coal combustion plasma with pre-heated, oxygen-enriched air, and potassium carbonate seed.

Fig 6.4 Isopleths of scalar electrical conductivity as a function of pressure and temperature for a typical coal combustion plasma with pre-heated, oxygen- enriched air, and potassium carbonate seed.

Fig. 6.5 Representation of multi-dimensional fluid and electrical phenomena in linear MHD generator ducts. General flow field involves swirling secondary flow resulting from combustor swirl and transverse Lorentz forces. Current distributions are concentrated at electrode edges due to Hall effects. Heat transfer and skin friction are strongly non-uniform due to current concentrations and arcs. In slagging generators, hydrodynamic slag films interact with the plasma.

Fig. 6.6 Effect of Hall current on pressure distribution between electrodes. Local Hall currents generate local transverse Lorentz forces which induce transverse pressure gradients.

A net Hall current leads to a pressure on the cathode wall which is greater than the anode wall pressure.

Fig. 6.7 Axial velocity profile development in an MHD generator of scale $S_U = 10$. Sidewall velocity overshoots occur because of cool boundary layer regions in which the current, and hence the Lorentz force, vanish.

Fig. 6.8 Skin-friction distributions on electrode and sidewalls for a typical high interaction MHD generator act with the plasma. Velocity overshoots on sidewalls lead to enhanced shear and skin friction.

Fig. 6.9 Development of the streamfunction formed from the vortical component of the secondary flows in the cross-section at $1m$ intervals in a $7m$ long MHD generator duct. Station locations are relative to the first loaded electrode.

Fig. 6.10 Full profile structure of axial velovity and vortical secondary flow component streamlines in a magnetoaerothermally unstable flow. Transverse Lorentz forces in the core resulting from the Hall effect and cool walls leads to the development of a set of vortical secondary flow cells. These cells convect hot fluid into the center of the anode which generates a further increase in the transverse Lorentz force and the plasma.

Fig. 6.11 MHD generator flow train with control points which induce transient effects.

Fig. 6.12 Amplitude-space-time representation of dynamic variables in transient flow train response. Any variable ϕ has an amplitude at any point in space x at time t which describes the strength of the disturbance. The projection of these amplitudes on the $x - t$ plane defines a trajectory whose slope is the propagation speed of any disturbance in the variable

Fig. 6.13 Response during the start-up transient of a large ($S_U \approx 10$) MHD generator flow train as manifested in the pressure. Initial pressure pulse from combustion heat release raises the combustor pressure to a peak of nealy $6atm$ at about $2ms$ after ignition. This pulse propagates through the combustor and is both reflected from the nozzle throat and transmitted downstream through the cold oxidizer flow. The downstream wave collides with the cold flow shock leading to further reflected and transmitted waves. The second combustion initiated wave propagates downstream in hot fluid overtaking and merging with the first. Hot, conducting fluid propagates through the system beginning at $7ms$ after ignition. Once conducting fluid enters the generator, the Lorentz force acts upon the

flow and the original cold flow shock (which exists since Lorentz forces are not present) is dispersed. Fluid speed is U; speed of sound is c.

Fig. 6.14 Hall field E_x response during the start-up transient of a large MHD flow train. Fields in excess of $4kV/m$ exist for a period of about $10-20ms$ over a large portion of the generator; such fields can result in axial breakdown arcs.

Fig. 7.1 Cutaway illustration of MK CA-1 accelerator and arc jet shown mounted on thrust stand. (Momentum change of stream is measured by observing thrust change on strain gages.)

Fig. 7.2 Cylindrical geometry MPD accelerator.

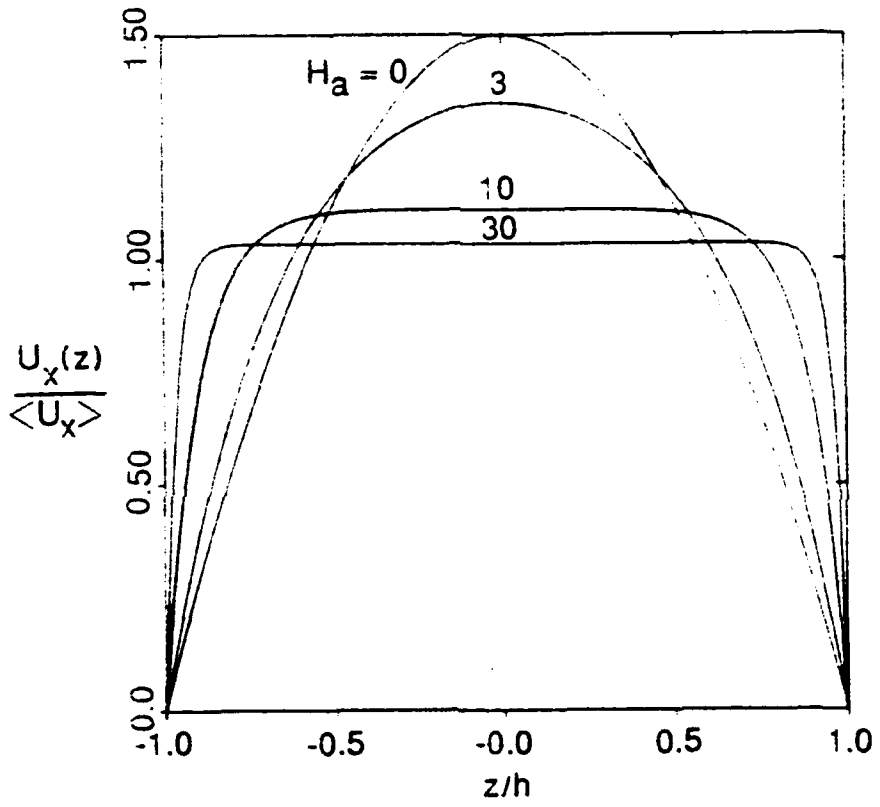
1.50
1.00
0.50
0.0
H_a = 0
3
10
30
$\frac{U_x(z)}{\langle U_x \rangle}$
-1.0
-0.5
-0.0
0.5
1.0
z/h

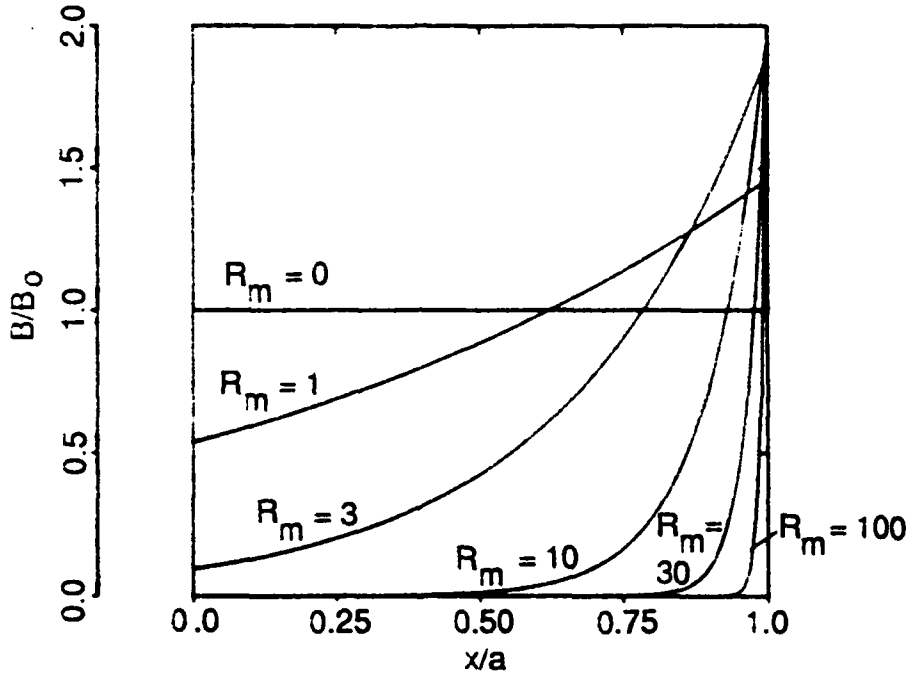
B/B$_o$
2.0
1.5
1.0
0.5
0.0
R$_m$ = 0
R$_m$ = 1
R$_m$ = 3
R$_m$ = 10
R$_m$= 30
R$_m$= 100
0.0
0.25
0.50
0.75
1.0
x/a

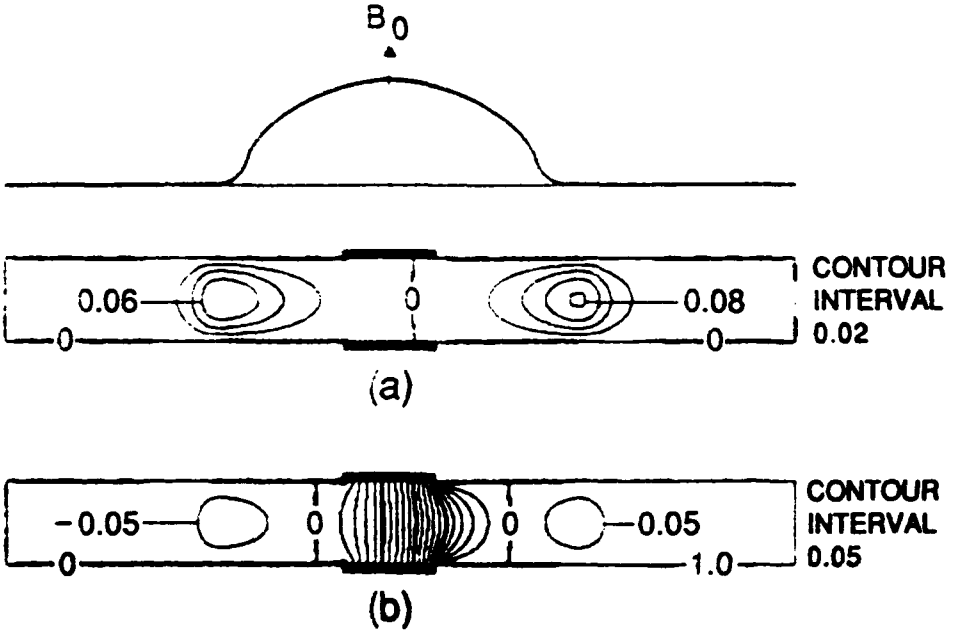
B_0
0.06
0
0
0.08
0
CONTOUR INTERVAL 0.02
(a)
-0.05
0
0
0.05
0
1.0
CONTOUR INTERVAL 0.05
(b)

5.2
4.2

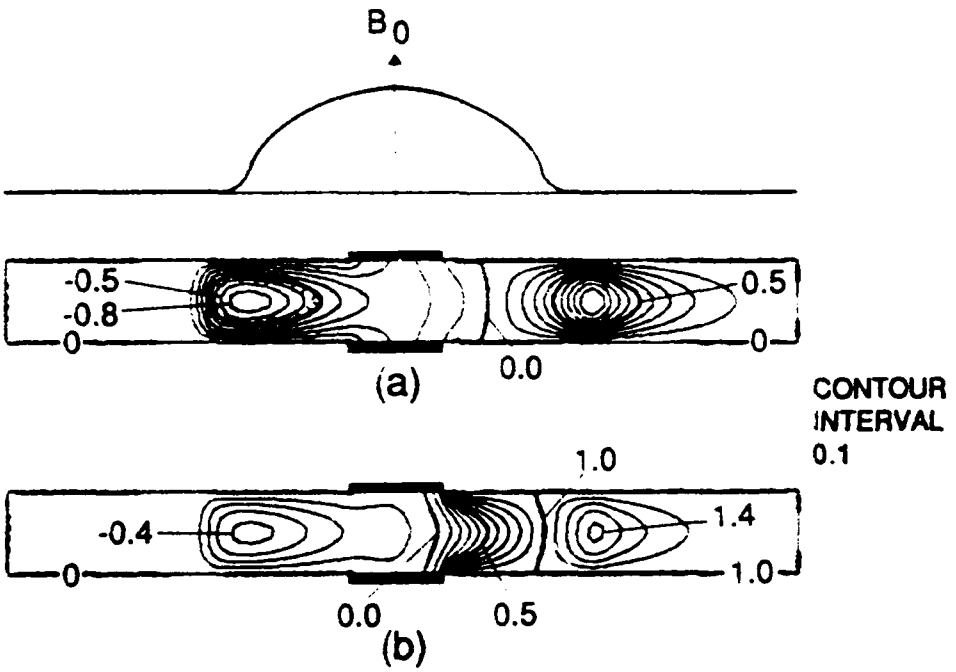

5.3
4 2

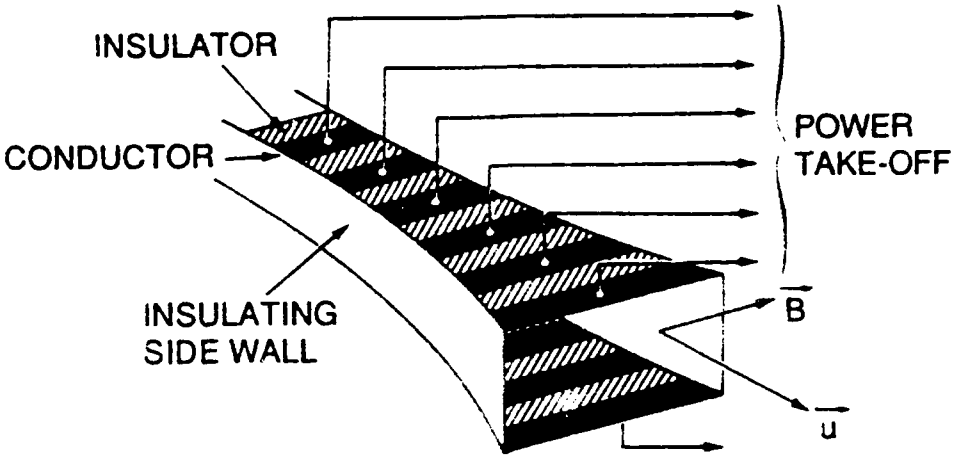
INSULATOR
CONDUCTOR
INSULATING
SIDE WALL
POWER
TAKE-OFF
B
u

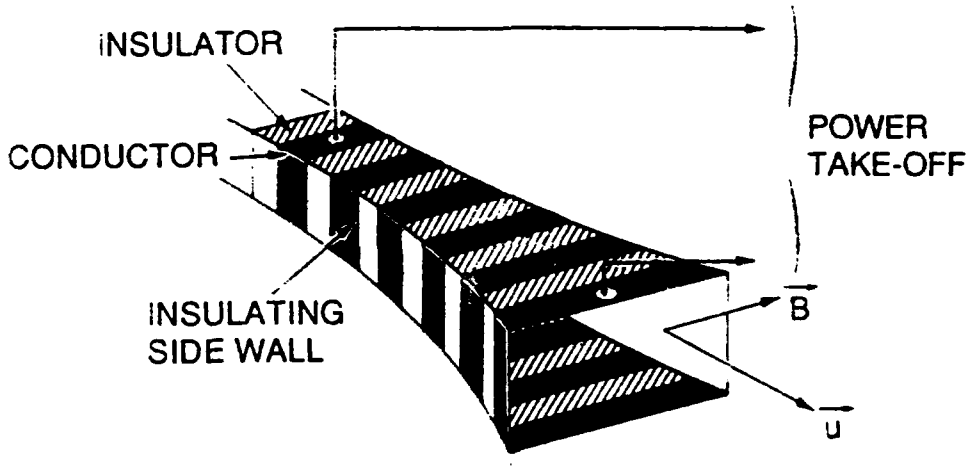
INSULATOR
CONDUCTOR
INSULATING
SIDE WALL
POWER
TAKE-OFF
B
u

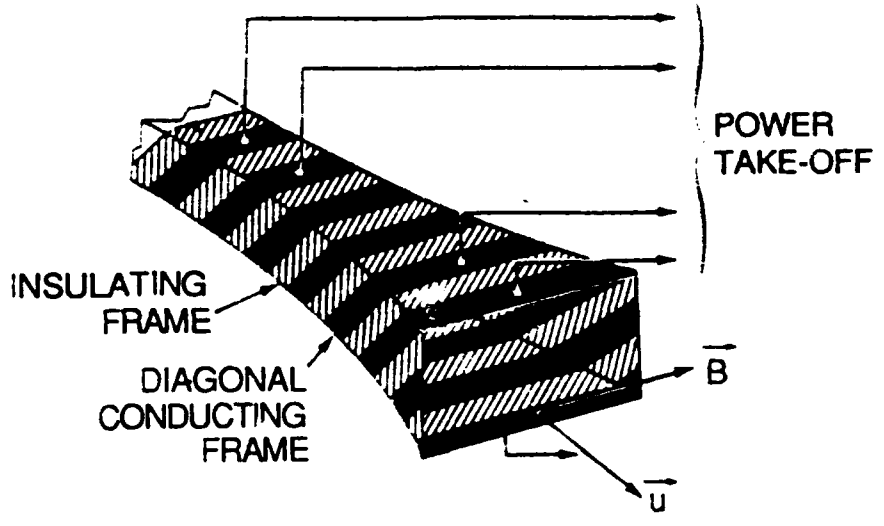
INSULATING
FRAME
DIAGONAL
CONDUCTING
FRAME
POWER
TAKE-OFF
B
u

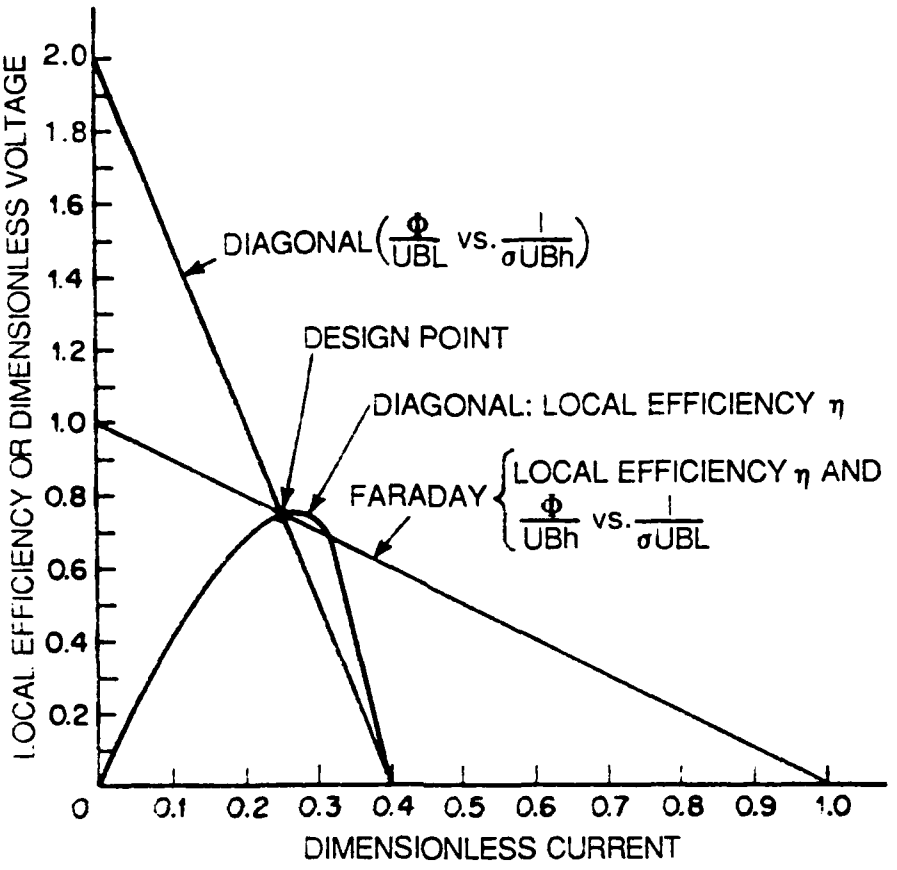
LOCAL EFFICIENCY OR DIMENSIONLESS VOLTAGE
2.0
1.8
1.6
1.4
1.2
1.0
0.8
0.6
0.4
0.2
0
0.1 0.2 0.3 0.4 0.5 0.6 0.7 0.8 0.9 1.0
DIMENSIONLESS CURRENT
DIAGONAL $\left(\frac{\Phi}{UBL} \text{ vs. } \frac{1}{\sigma UBh}\right)$
DESIGN POINT
DIAGONAL: LOCAL EFFICIENCY η
FARADAY
LOCAL EFFICIENCY η AND $\frac{\Phi}{UBh}$ vs. $\frac{1}{\sigma UBL}$

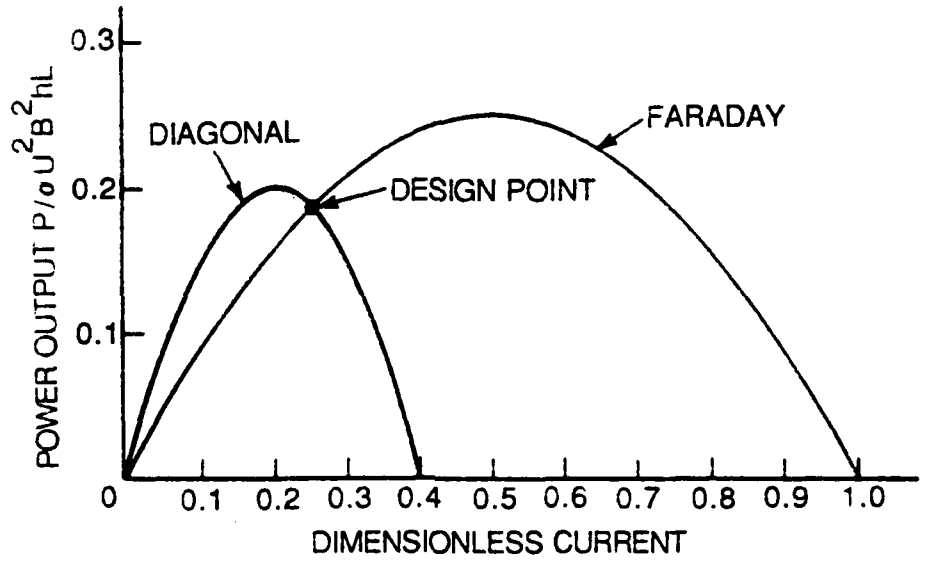
POWER OUTPUT $P/\sigma U^2 B^2 hL$
0.3
0.2
0.1
0
0.1 0.2 0.3 0.4 0.5 0.6 0.7 0.8 0.9 1.0
DIMENSIONLESS CURRENT
DIAGONAL
FARADAY
DESIGN POINT

6.2

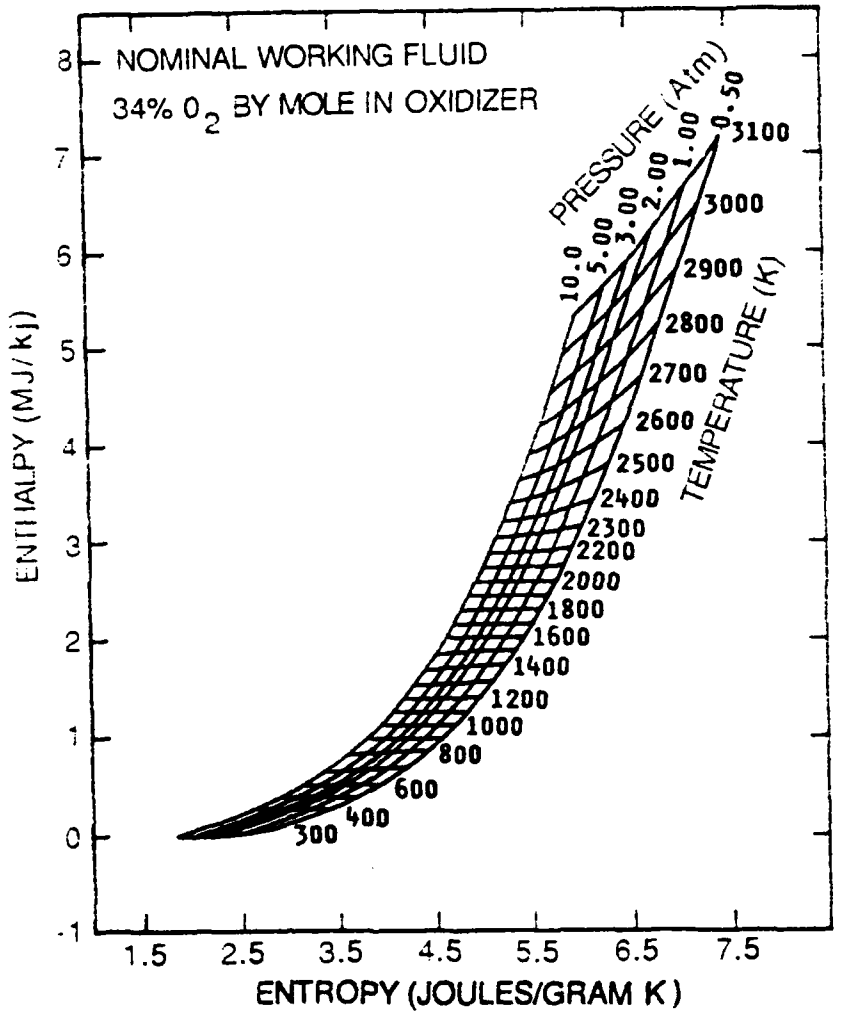
NOMINAL WORKING FLUID
34% O_2 BY MOLE IN OXIDIZER
PRESSURE (Atm)
0.50
1.00
2.00
3.00
5.00
10.0
TEMPERATURE (K)
3100
3000
2900
2800
2700
2600
2500
2400
2300
2200
2000
1800
1600
1400
1200
1000
800
600
400
300
ENTHALPY (MJ/kj)
8
7
6
5
4
3
2
1
0
-1
1.5
2.5
3.5
4.5
5.5
6.5
7.5
ENTROPY (JOULES/GRAM K)

6.3

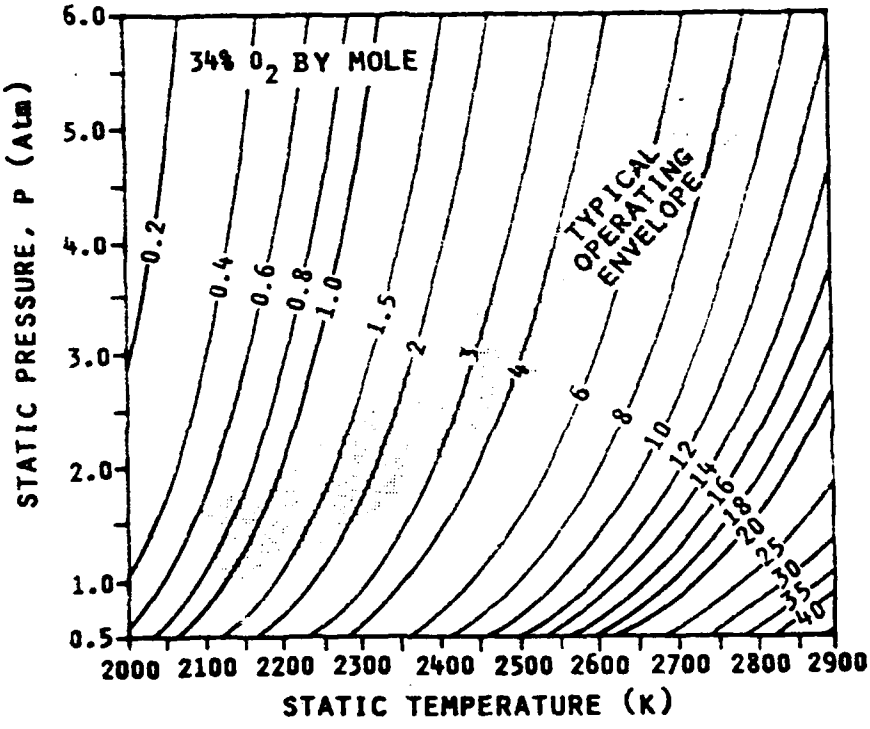
34% O_2 BY MOLE
TYPICAL OPERATING ENVELOPE
0.2
0.4
0.6
0.8
1.0
1.5
2
3
4
6
8
10
12
14
16
18
20
25
30
35
40
STATIC PRESSURE, P (Atm)
6.0
5.0
4.0
3.0
2.0
1.0
0.5
2000 2100 2200 2300 2400 2500 2600 2700 2800 2900
STATIC TEMPERATURE (K)

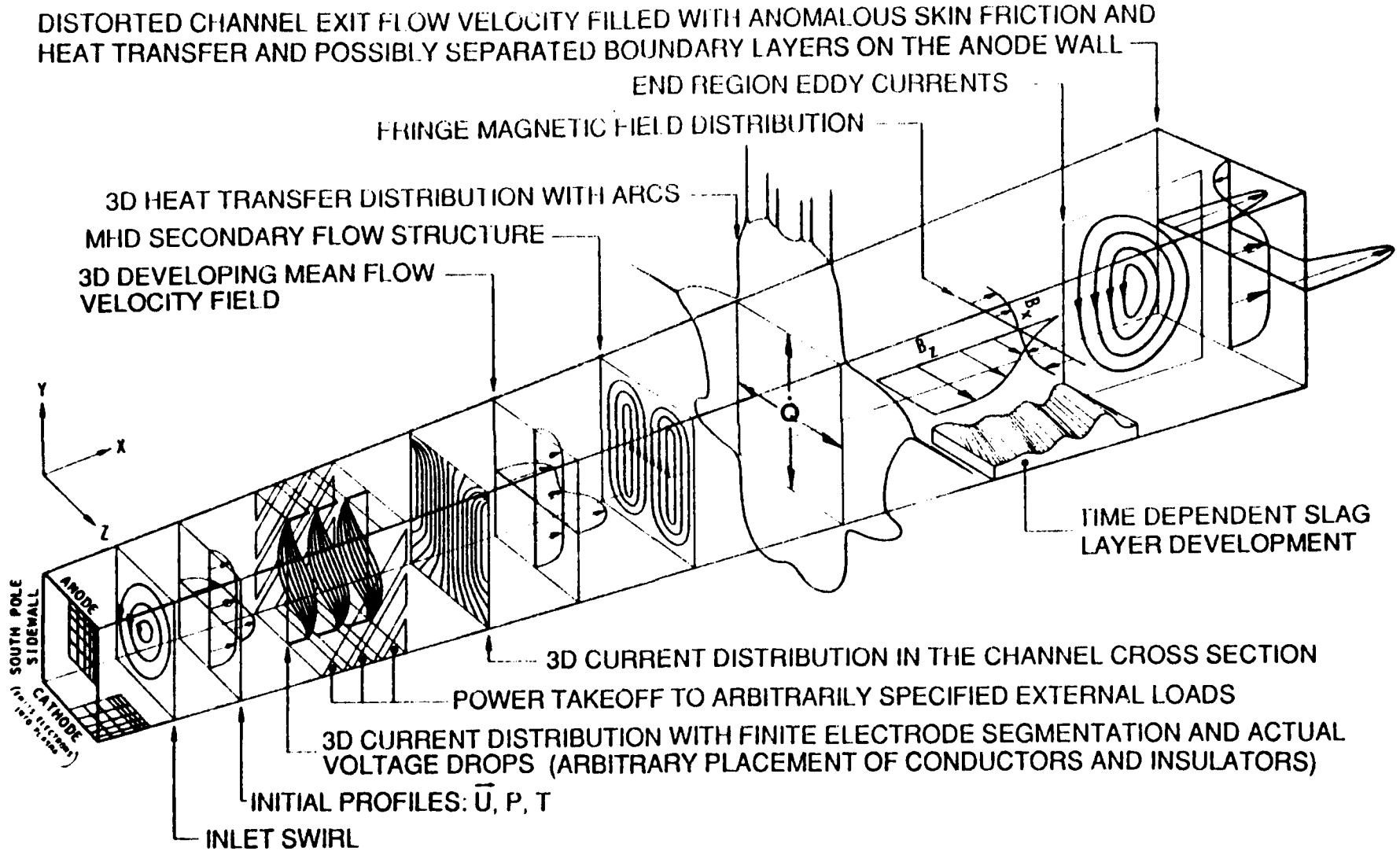
DISTORTED CHANNEL EXIT FLOW VELOCITY FILLED WITH ANOMALOUS SKIN FRICTION AND HEAT TRANSFER AND POSSIBLY SEPARATED BOUNDARY LAYERS ON THE ANODE WALL
END REGION EDDY CURRENTS
FRINGE MAGNETIC FIELD DISTRIBUTION
3D HEAT TRANSFER DISTRIBUTION WITH ARCS
MHD SECONDARY FLOW STRUCTURE
3D DEVELOPING MEAN FLOW VELOCITY FIELD
Y
X
Z
$\dot{Q}$
B_x
B_z
SOUTH POLE SIDEWALL
ANODE
CATHODE
TIME DEPENDENT SLAG LAYER DEVELOPMENT
3D CURRENT DISTRIBUTION IN THE CHANNEL CROSS SECTION
POWER TAKEOFF TO ARBITRARILY SPECIFIED EXTERNAL LOADS
3D CURRENT DISTRIBUTION WITH FINITE ELECTRODE SEGMENTATION AND ACTUAL VOLTAGE DROPS (ARBITRARY PLACEMENT OF CONDUCTORS AND INSULATORS)
INITIAL PROFILES: $\vec{U}$, P, T
INLET SWIRL

5.9

TRANSVERSE LORENTZ FORCE EFFECTS

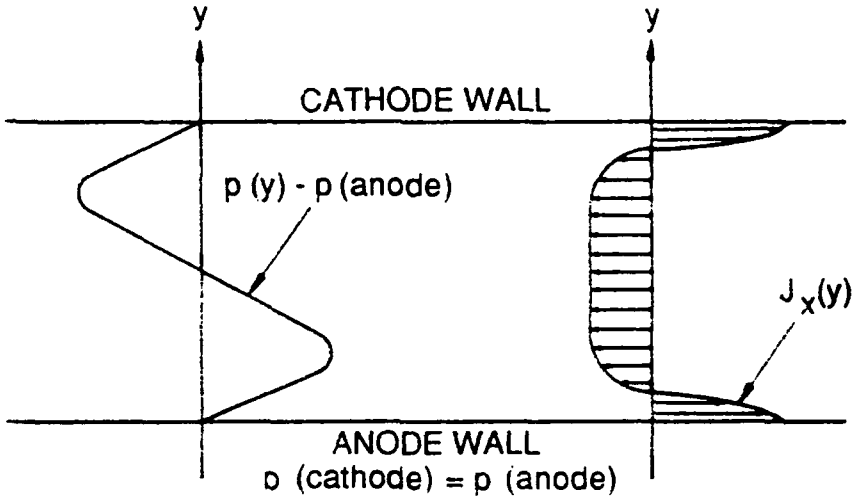

FARADAY CONNECTION: $I_x = \int J_x dy = 0$

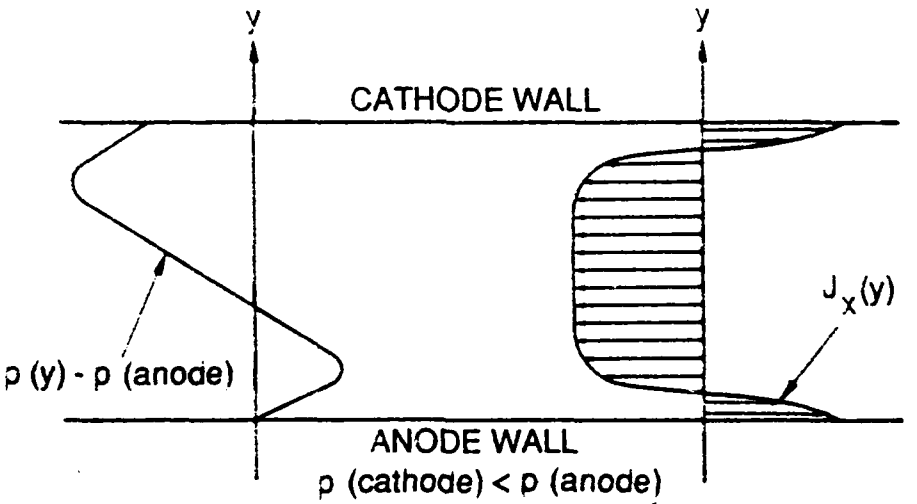

NON-ZERO AXIAL CURRENT : $\int J_x dy < 0$

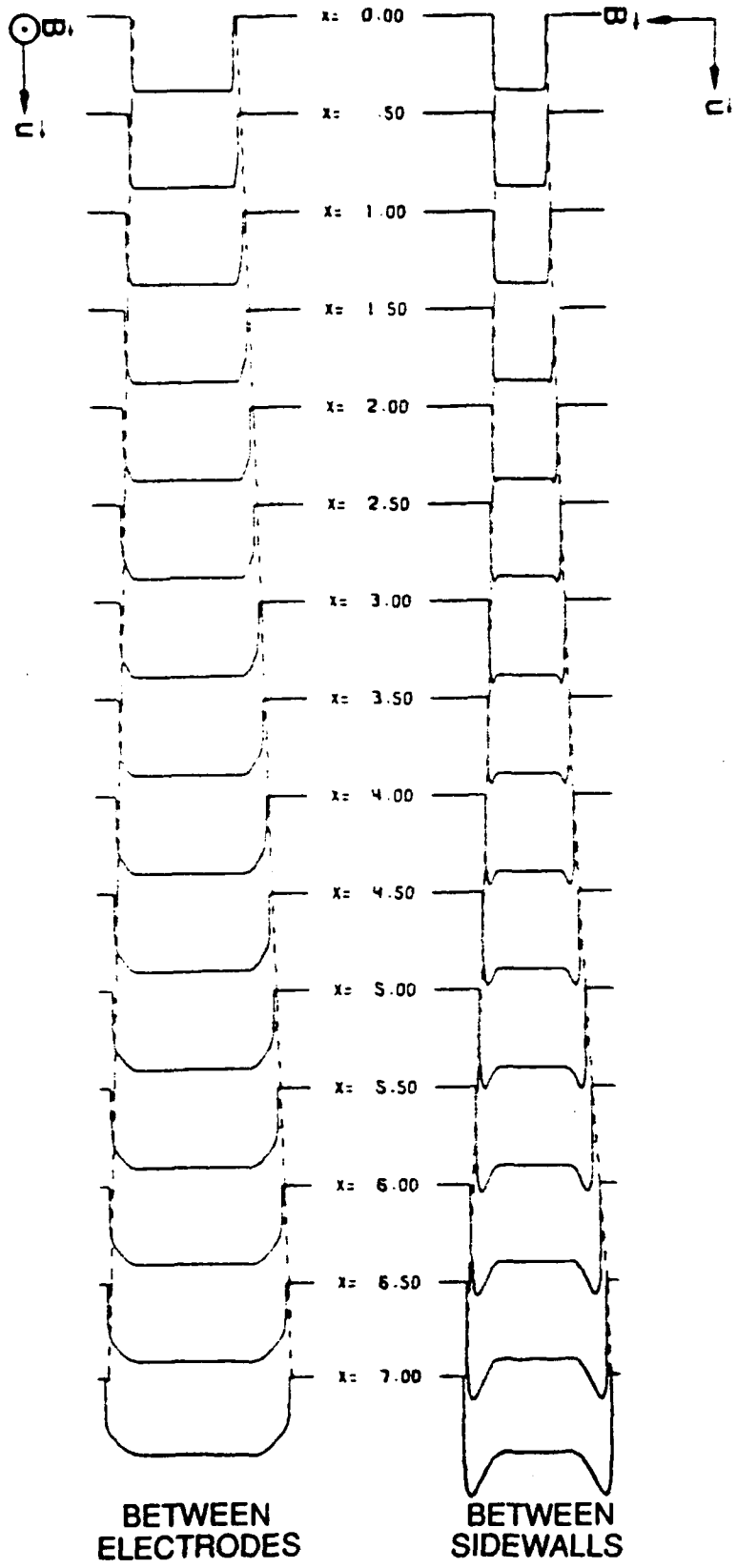
x= 0.00
x= .50
x= 1.00
x= 1.50
x= 2.00
x= 2.50
x= 3.00
x= 3.50
x= 4.00
x= 4.50
x= 5.00
x= 5.50
x= 6.00
x= 6.50
x= 7.00
BETWEEN ELECTRODES
BETWEEN SIDEWALLS

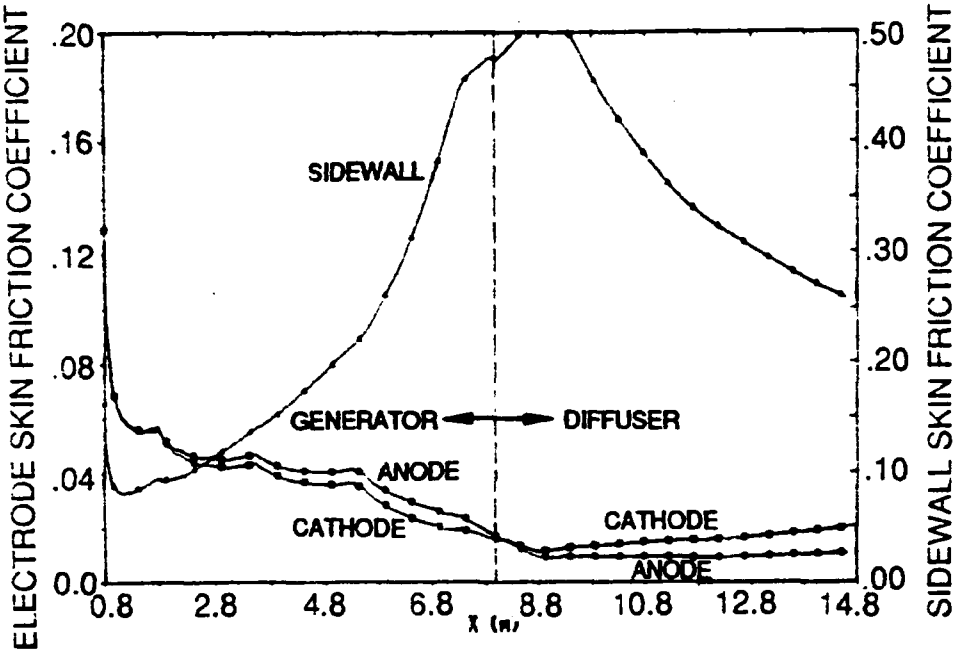
ELECTRODE SKIN FRICTION COEFFICIENT
SIDEWALL SKIN FRICTION COEFFICIENT
.20
.16
.12
.08
.04
0.0
.50
.40
.30
.20
.10
.00
0.8
2.8
4.8
6.8
8.8
10.8
12.8
14.8
X (m)
SIDEWALL
GENERATOR
DIFFUSER
ANODE
CATHODE
CATHODE
ANODE

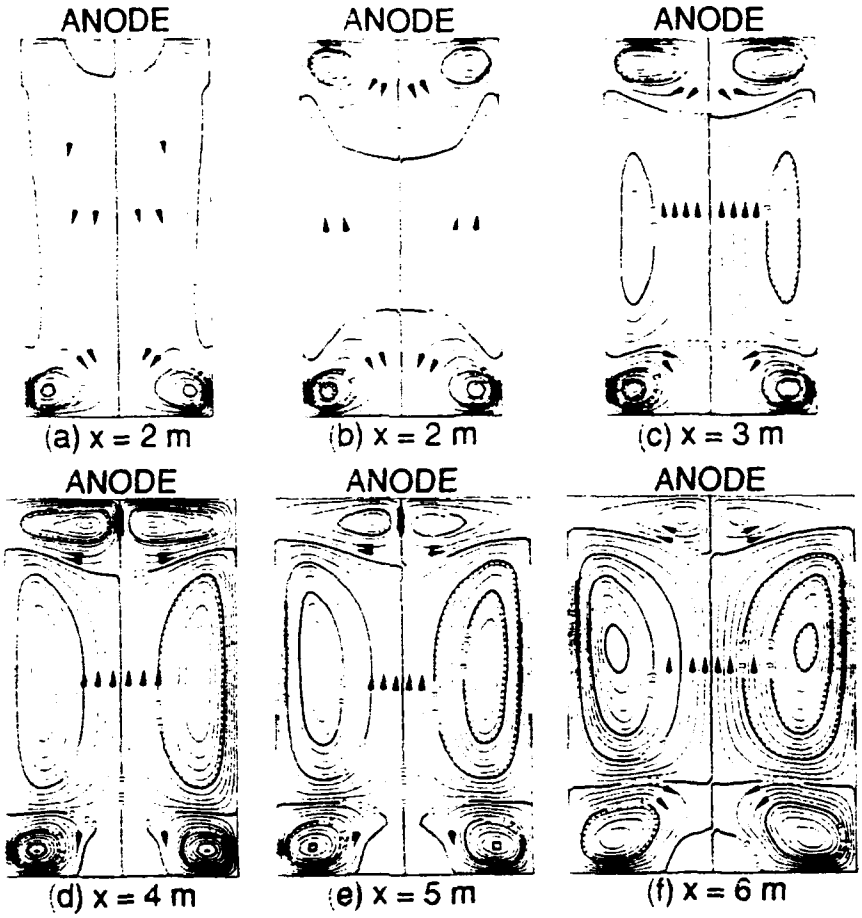
ANODE
ANODE
ANODE
(a) x = 2 m
(b) x = 2 m
(c) x = 3 m
ANODE
ANODE
ANODE
(d) x = 4 m
(e) x = 5 m
(f) x = 6 m

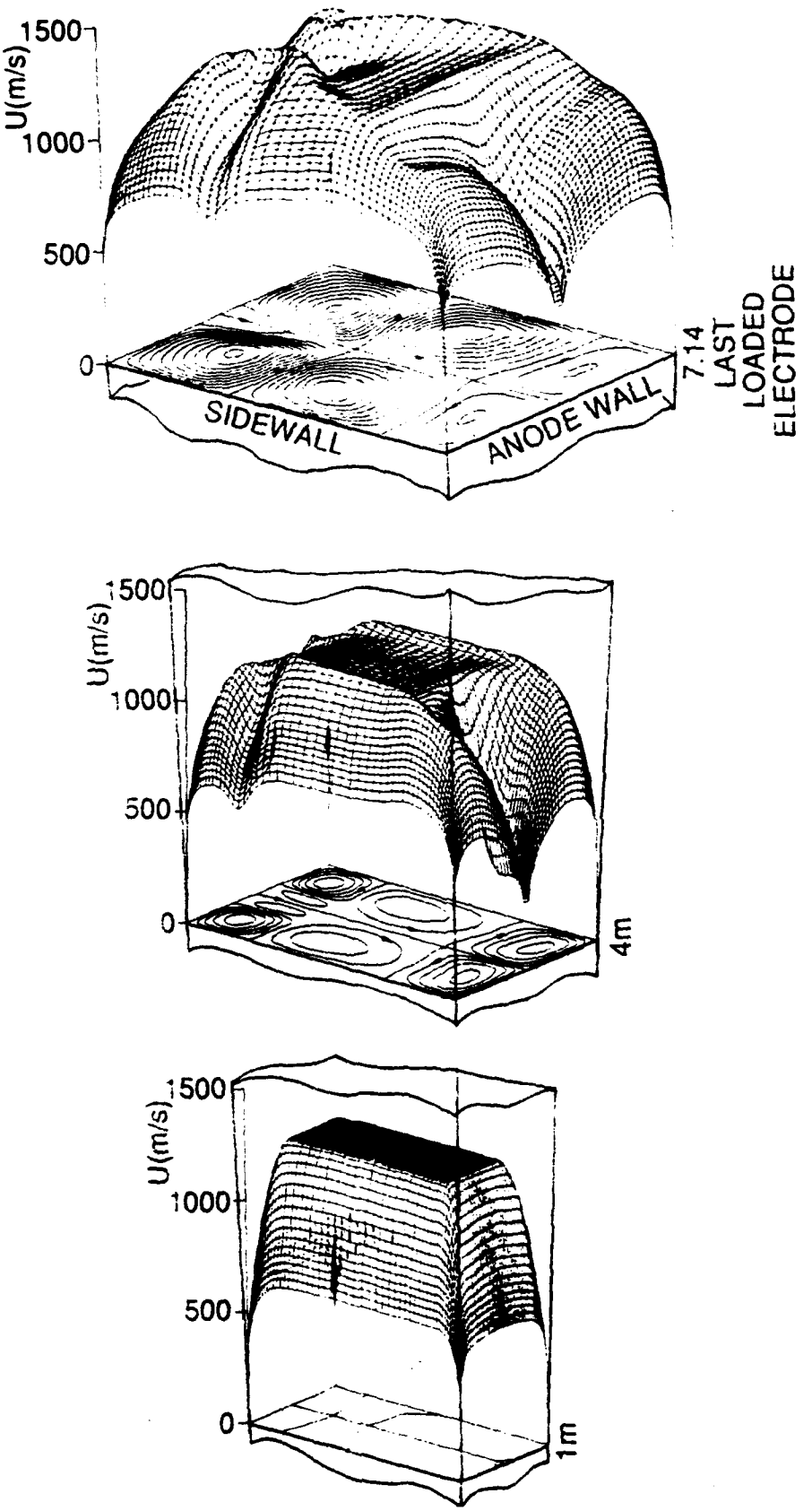
U(m/s)
1500
1000
500
0
SIDEWALL
ANODE WALL
7.14
LAST
LOADED
ELECTRODE
U(m/s)
1500
1000
500
0
4m
U(m/s)
1500
1000
500
0
1m

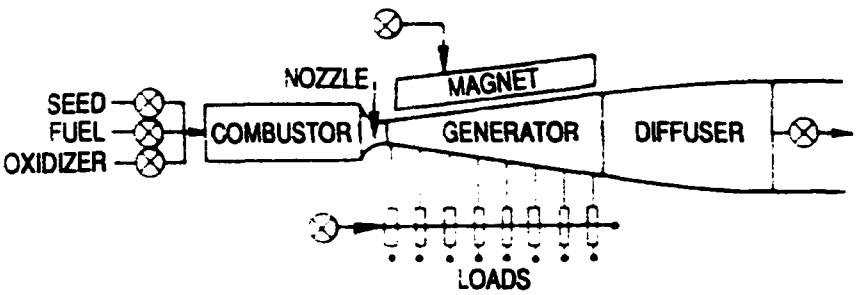

⊗ DENOTES TYPICAL CONTROL POINTS IN THE FLOWTRAIN

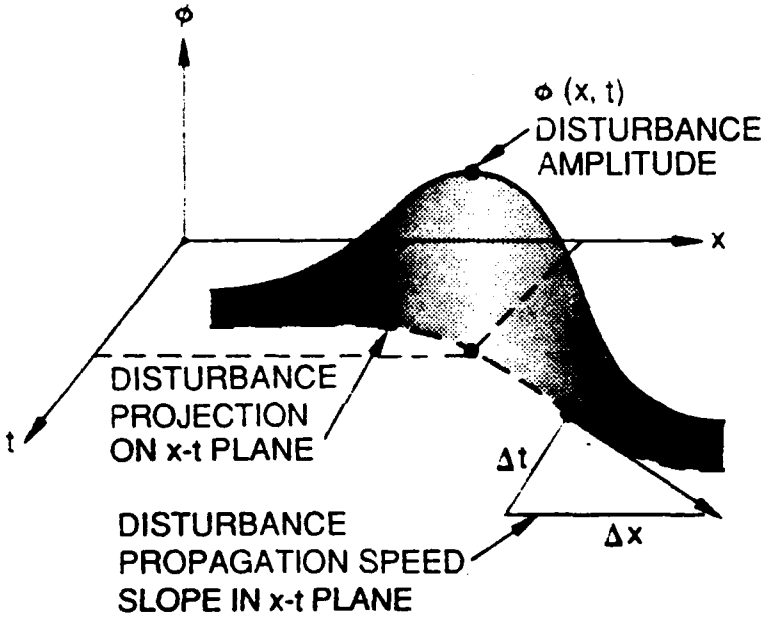
φ
φ (x, t)
DISTURBANCE
AMPLITUDE
x
t
DISTURBANCE
PROJECTION
ON x-t PLANE
Δt
Δx
DISTURBANCE
PROPAGATION SPEED
SLOPE IN x-t PLANE

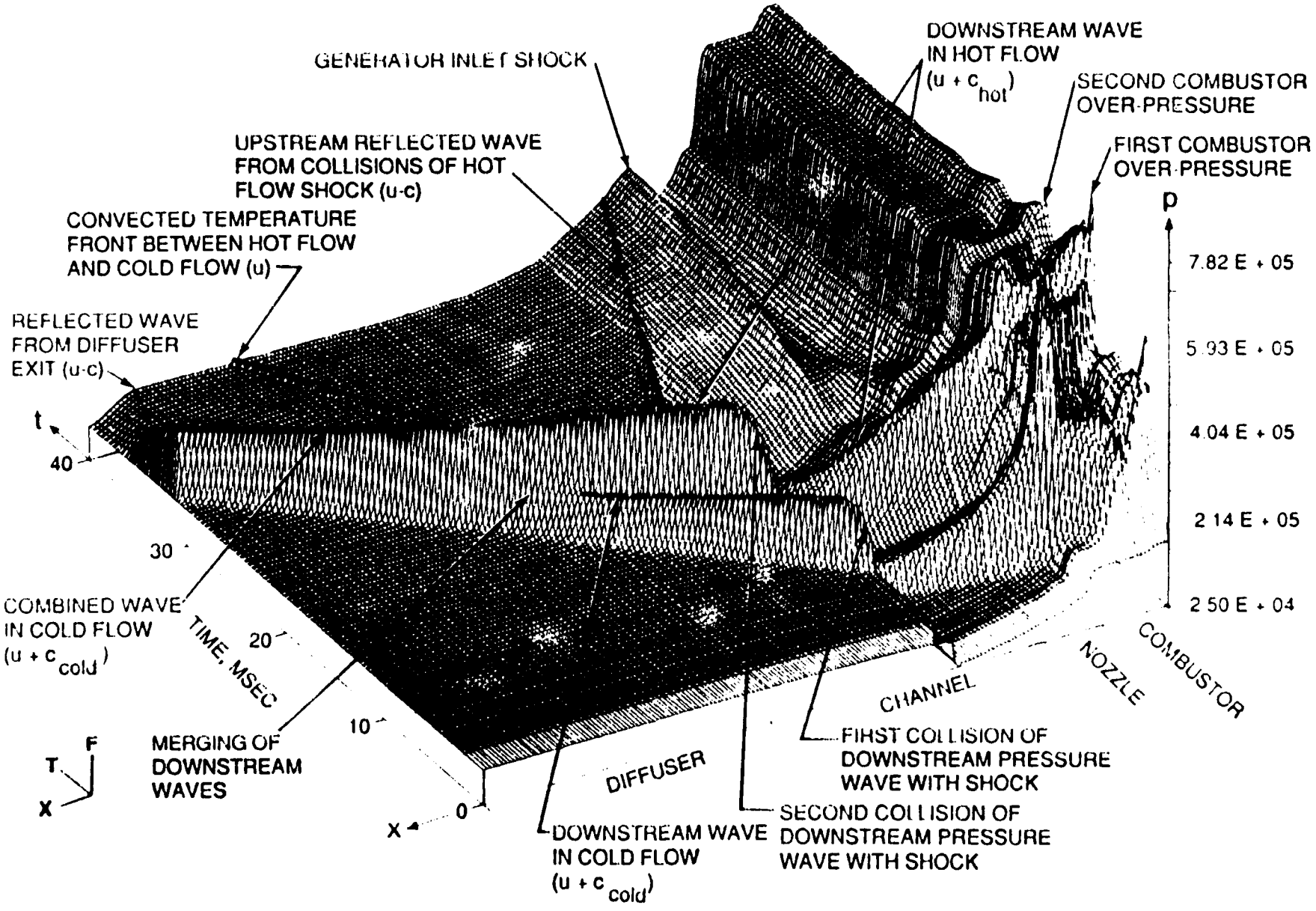
GENERATOR INLET SHOCK
DOWNSTREAM WAVE IN HOT FLOW (u + c hot)
SECOND COMBUSTOR OVER-PRESSURE
FIRST COMBUSTOR OVER-PRESSURE
UPSTREAM REFLECTED WAVE FROM COLLISIONS OF HOT FLOW SHOCK (u-c)
CONVECTED TEMPERATURE FRONT BETWEEN HOT FLOW AND COLD FLOW (u)
REFLECTED WAVE FROM DIFFUSER EXIT (u-c)
p
7.82 E + 05
5.93 E + 05
4.04 E + 05
2.14 E + 05
2.50 E + 04
t
40
30
20
10
0
TIME, MSEC
X
COMBINED WAVE IN COLD FLOW (u + c cold)
MERGING OF DOWNSTREAM WAVES
T
F
X
DIFFUSER
CHANNEL
NOZZLE
COMBUSTOR
FIRST COLLISION OF DOWNSTREAM PRESSURE WAVE WITH SHOCK
SECOND COLLISION OF DOWNSTREAM PRESSURE WAVE WITH SHOCK
DOWNSTREAM WAVE IN COLD FLOW (u + c cold)

6/13

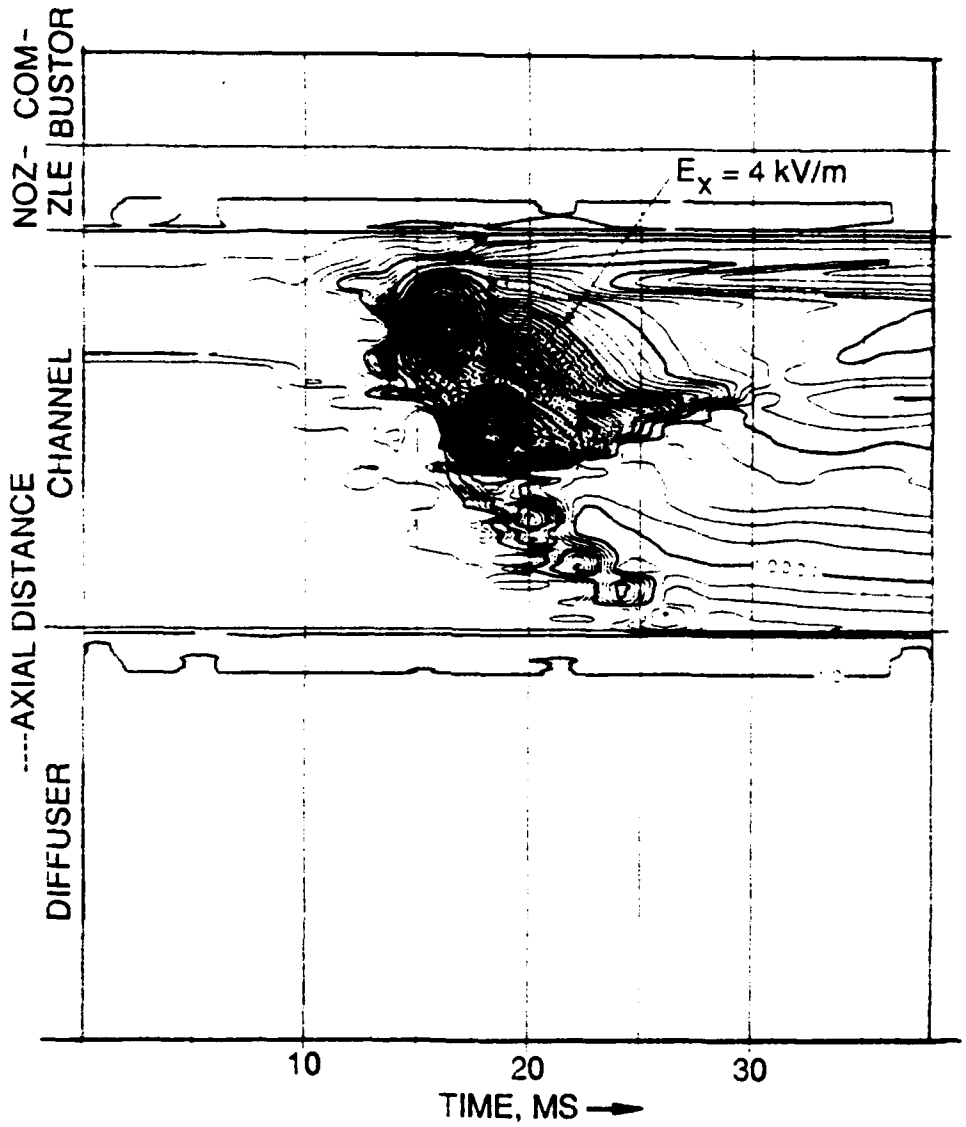
NOZ- ZLE
COM- BUSTOR
E_x = 4 kV/m
CHANNEL
---AXIAL DISTANCE
DIFFUSER
10
20
30
TIME, MS

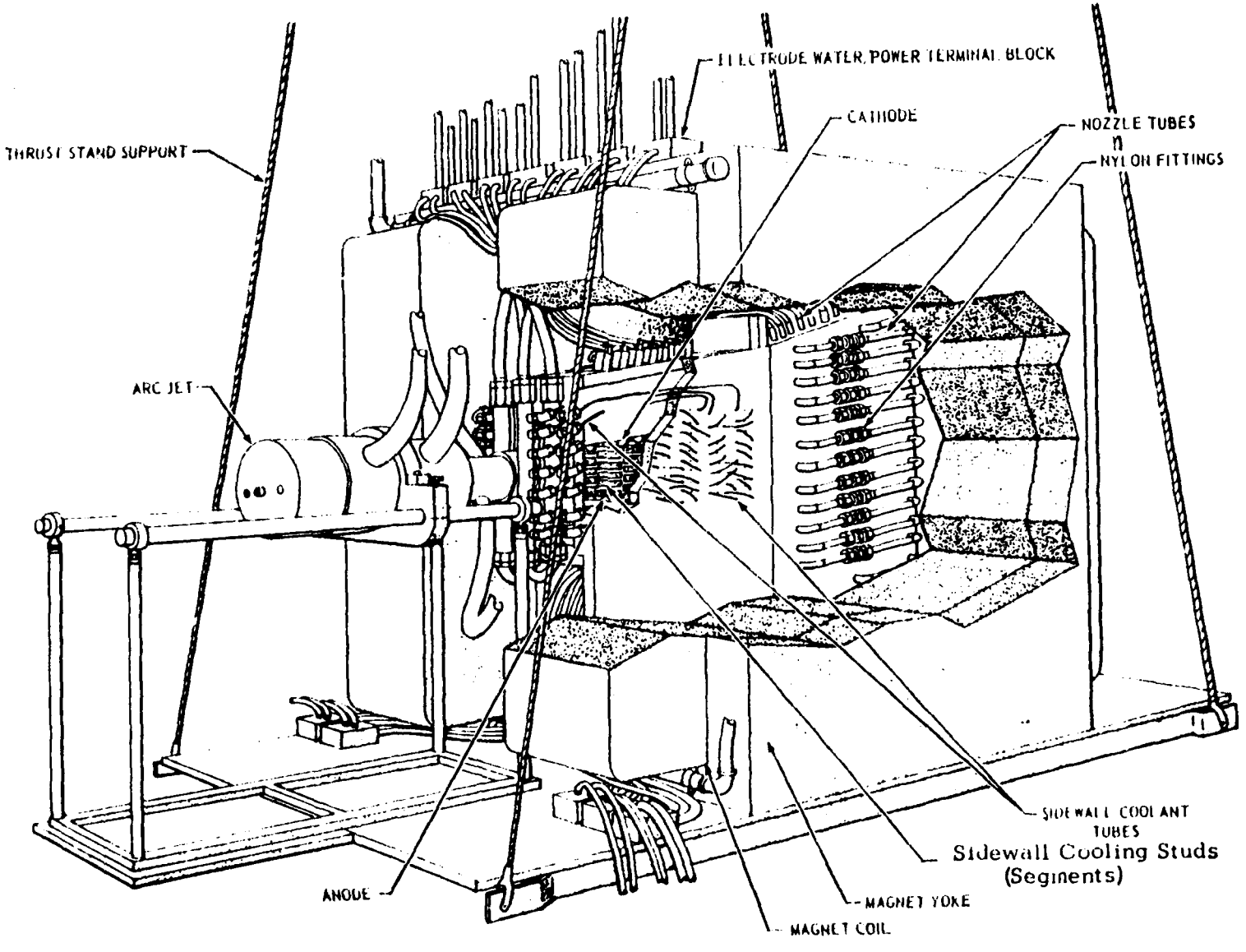
ELECTRODE WATER, POWER TERMINAL BLOCK
CATHODE
NOZZLE TUBES
NYLON FITTINGS
THRUST STAND SUPPORT
ARC JET
SIDEWALL COOLANT TUBES
Sidewall Cooling Studs (Segments)
ANODE
MAGNET YOKE
MAGNET COIL